From the Classical Frenet-Serret Apparatus to the Curvature and Torsion of Quantum-Mechanical Evolutions. Part I. Stationary Hamiltonians

Paul M. Alsing[1] and Carlo Cafaro[2,3]

[1]*Air Force Research Laboratory, Information Directorate, Rome, NY 13441, USA*
[2]*University at Albany-SUNY, Albany, NY 12222, USA and*
[3]*SUNY Polytechnic Institute, Utica, NY 13502, USA*

It is known that the Frenet-Serret apparatus of a space curve in three-dimensional Euclidean space determines the local geometry of curves. In particular, the Frenet-Serret apparatus specifies important geometric invariants, including the curvature and the torsion of a curve. It is also acknowledged in quantum information science that low complexity and high efficiency are essential features to achieve when cleverly manipulating quantum states that encode quantum information about a physical system.

In this paper, we propose a geometric perspective on how to quantify the bending and the twisting of quantum curves traced by dynamically evolving state vectors. Specifically, we propose a quantum version of the Frenet-Serret apparatus for a quantum trajectory in projective Hilbert space traced by a parallel-transported pure quantum state evolving unitarily under a stationary Hamiltonian specifying the Schrödinger equation. Our proposed constant curvature coefficient is given by the magnitude squared of the covariant derivative of the tangent vector $|T\rangle$ to the state vector $|\Psi\rangle$ and represents a useful measure of the bending of the quantum curve. Our proposed constant torsion coefficient, instead, is defined in terms of the magnitude squared of the projection of the covariant derivative of the tangent vector $|T\rangle$, orthogonal to both $|T\rangle$ and $|\Psi\rangle$. The torsion coefficient provides a convenient measure of the twisting of the quantum curve. Remarkably, we show that our proposed curvature and torsion coefficients coincide with those existing in the literature, although introduced in a completely different manner. Interestingly, not only we establish that zero curvature corresponds to unit geodesic efficiency during the quantum transportation in projective Hilbert space, but we also find that the concepts of curvature and torsion help enlighten the statistical structure of quantum theory. Indeed, while the former concept can be essentially defined in terms of the concept of kurtosis, the positivity of the latter can be regarded as a restatement of the well-known Pearson inequality that involves both the concepts of kurtosis and skewness in mathematical statistics. Finally, not only do we present illustrative examples with nonzero curvature for single-qubit time-independent Hamiltonian evolutions for which it is impossible to generate torsion, but we also discuss physical applications extended to two-qubit stationary Hamiltonians that generate curves with both nonzero curvature and nonvanishing torsion traced by quantum states with different degrees of entanglement, ranging from separable states to maximally entangled Bell states. In an appendix, we examine the different curvature and torsion characteristics of the three qubit $|GHZ\rangle$ and $|W\rangle$ states under evolution by a quantum Heisenberg Hamiltonian.

I. INTRODUCTION

Geometric reasoning is a powerful tool in theoretical physics to improve our description and, to a certain extent, to sharpen our comprehension of physical phenomena in both classical and quantum settings by providing deep physical insights [1]. For instance, it is acknowledged that the classical Frenet-Serret apparatus of a space curve in three-dimensional Euclidean space determines the local geometry of curves and specifies important geometric invariants, including the curvature and the torsion of a curve [2]. In classical mechanics, the concepts of curvature and torsion introduced within the Frenet-Serret apparatus can be helpful in studying geometric properties of classical Newtonian trajectories of a particle. For instance, curvature and torsion can be used to specify the geometry of the cylindrical helix motion of an electron in a homogeneous external magnetic field [3]. It is also known that the clever manipulation of quantum states that encode quantum information about a physical system is an extremely valuable skill in quantum information science [4]. In quantum mechanics, motivated by the problem of parameter estimation, the concept of curvature of a quantum Schrödinger trajectory was originally introduced in Ref. [5] as a generalization of the notion of curvature of a classical exponential family of distributions of relevance to statistical mechanics. In the context of geometry of quantum statistical inference of Ref. [5], the curvature of a curve can be expressed in terms of the suitably defined squared acceleration vector of the curve and is a measure of the parametric sensitivity [6] that specifies the particular parametric estimation problem being under consideration. In Ref. [7], instead, Laba and Tkachuk proposed a definition of both curvature and torsion of quantum evolutions for pure quantum state undergoing a time-independent

Hamiltonian evolution. In their work, focusing on single-qubit quantum states, curvature measured the deviation of the dynamically evolving state vector from the geodesic line on the Bloch sphere. Instead, their proposed torsion concept quantified the deviation of the dynamically evolving state vector from a two-dimensional subspace specified by the instantaneous plane of evolution. Interestingly, building on the formalism developed in Ref. [7], the concepts of curvature and torsion have been recently used to study the geometric properties of different types of graph states of spin systems evolving under Ising-like interactions in Ref. [8].

In this paper, we are interested in quantifying the concepts of curvature and torsion of a quantum trajectory for several reasons. First, we are interested in understanding how to *bend* and *twist* quantum-mechanical evolutions of quantum states that encode relevant quantum information about the physical systems being observed. This is not only important from a conceptual standpoint, it can also be especially relevant in experimental quantum laboratory settings [9, 10]. Second, we are interested in comprehending the possible link between the curvature (and/or the torsion) and the complexity of a path traced out by a quantum state driven from a source state to a target state [11, 12]. Finally, we are interested in finding out if we can suitably manipulate via bending and twisting a trajectory traced out by a quantum state in an efficient manner so that one optimizes the travel time, maximizes the speed of evolution and, possibly, minimizes possible dissipative effects of thermodynamical origin that can emerge in the physical system being analyzed [13–15].

In this paper, we present a geometric approach to characterize the *bending* and the *twisting* of quantum curves traced out by evolving state vectors. More precisely, we offer a quantum version of the classical Frenet-Serret apparatus for a quantum trajectory on the Bloch sphere traced out by a parallel-transported pure quantum state developing unitarily subject to a time-independent Hamiltonian that specifies the Schrödinger equation. Indeed, we remark that our formalism is not limited to single-qubit two-dimensional complex Hilbert spaces and to quantum curves on the standard Bloch sphere $\mathbb{C}P^1 = \mathcal{S}^3/\mathcal{S}^1 = \mathcal{S}^2$ with $\mathcal{S}^k$ denoting the k-sphere. Instead, it applies in principle to any N-dimensional complex Hilbert space and to quantum curves on generalized "Bloch spheres" $\mathbb{C}P^{N-1} = \mathcal{S}^{2N-1}/\mathcal{S}^1$ [16]. We propose a curvature coefficient defined as the magnitude squared of the covariant derivative of the tangent vector to the state vector and represents a suitable measure of the bending of the quantum curve. We also suggest a concept of torsion coefficient, instead, specified by means of the magnitude squared of the projection of the covariant derivative of the tangent vector, orthogonal to the state vector as well as to the tangent vector to the state vector. Our proposed torsion coefficient is a good measure of the twisting of the quantum curve. Remarkably, as a by-product, we demonstrate that our proposed curvature and torsion coefficients are identical to those proposed by Laba and Tkachuk in Ref. [7], although we justify our proposals inspired by the classical Frenet-Serret apparatus. Finally, not only we consider illustrative examples for pedagogical purposes, we also discuss the generalization of our theoretical construct to time-dependent quantum-mechanical scenarios where both curvature and torsion coefficients play a key role.

The layout of the rest of this paper is as follows. In Sec. II, we present some background material that focuses on the curvature and torsion coefficients of a quantum evolution as originally proposed by Laba and Tkachuk in Ref. [7]. In Sec. III, in preparation of our newly proposed theoretical construct in Sec. IV, we recall the essential ingredients of a classical Frenet-Serret apparatus with special emphasis on the notions of bending and twisting as captured by the curvature and the torsion of a curve in three-dimensional Euclidean space. In Sec. IV, we present our quantum version of the classical Frenet-Serret apparatus suitable for quantifying the bending and the twisting of a quantum curve traced out by a parallel-transported unit state vector that evolves under the action of a time-independent Hamiltonian. Remarkably, although obtained from an alternative perspective that mimics a classical apparatus, we find that our proposed curvature and torsion coefficients coincide with the ones proposed by Laba and Tkachuk in Ref. [7]. In Sec. V, we present several points of discussion. First, we discuss the statistical interpretation of the curvature and torsion coefficients. Second, we illustrate the usefulness of recasting the expressions of these two coefficients in terms of the Bloch vector for two-level systems. Third, we elaborate on several challenges that can emerge in higher-dimensional Hilbert spaces with quantum evolutions governed by nonstationary Hamiltonians. Finally, we present in Sec. V a comparison between our proposed quantum apparatus and the classical Frenet-Serret one. In Sec. VI, we demonstrate simple illustrative examples of the behavior of curvature and torsion coefficients for quantum evolutions specified by single-qubit and two-qubit time-independent Hamiltonians. In Section VII, we present our conclusive remarks. Finally, an illustrative example on how to frame a quantum curve can be found in Appendix A, a link between the concept of geodesic curvature [17–19] and our proposed curvature coefficient appears in Appendix B and, lastly, in Appendix C we report on the behavior of curvature and torsion coefficients for quantum curves traced by three-qubit quantum states evolving under a quantum Heisenberg model Hamiltonian.

II.   THE QUANTUM LABA-TKACHUK FRAMEWORK

In this section, we report on some relevant background material that puts the emphasis on how to introduce suitable measures of curvature and torsion of a quantum evolution. Specifically, we revisit the work that was originally proposed by Laba and Tkachuk in Ref. [7].

A.   Curvature

In Ref. [7], Laba and Tkachuk propose a concept of curvature coefficient for a Schrödinger quantum-mechanical evolution specified by a time-independent Hamiltonian H. The curvature coefficient proposed in Ref. [7] emerges by quantifying the departure of the unit evolution vector $|\psi(t)\rangle = e^{(-i/\hbar)Ht}|\psi(0)\rangle$ with $0 \leq t \leq t_f$ from the geodesic path $|\psi(\xi)\rangle$ connecting the initial state $|\psi(0)\rangle \overset{\text{def}}{=} |\psi_i\rangle$ and the final state $|\psi(t_f)\rangle \overset{\text{def}}{=} |\psi_f\rangle$. The real parameter $\xi \in [0, 1]$ and $|\psi(\xi)\rangle$ is given by [7],

$$|\psi(\xi)\rangle \overset{\text{def}}{=} \frac{1}{\sqrt{1 - 2\xi(1-\xi)(1 - |\langle\psi_f|\psi_i\rangle|)}} \left[(1-\xi)|\psi_i\rangle + \xi\frac{\langle\psi_f|\psi_i\rangle}{|\langle\psi_f|\psi_i\rangle|}\right]|\psi_f\rangle. \tag{1}$$

More specifically, the focus about the temporal evolution that occurs during the temporal interval $[0, t_f]$ is on two stages. In the first stage, the state evolves from $|\psi(0)\rangle$ to $|\psi(\Delta t)\rangle = e^{(-i/\hbar)H\Delta t}|\psi(0)\rangle$ with $0 \leq \Delta t \leq t_f$. In the second stage, the state evolves from $|\psi(\Delta t)\rangle$ to $|\psi(\Delta t + \Delta t')\rangle = e^{(-i/\hbar)H(\Delta t + \Delta t')}|\psi(0)\rangle = e^{(-i/\hbar)H\Delta t'}|\psi(\Delta t)\rangle$ with $\Delta t' \geq 0$ and $0 \leq \Delta t + \Delta t' \leq t_f$. Then, setting $\Delta t' = \Delta t$ for simplicity, Laba and Tkachuk argue that a departure of the actual quantum-mechanical evolution from the geodesic evolution from $|\psi_i\rangle$ to $|\psi_f\rangle$ can be detected by considering the minimal squared distance $d_{\min}^2$ between $|\psi(\Delta t)\rangle$ and $|\psi(\xi)\rangle$ in Eq. (1),

$$d_{\min}^2 \overset{\text{def}}{=} \min_{0 \leq \xi \leq 1} d^2(\xi) = \min_{0 \leq \xi \leq 1}\left\{\gamma^2\left[1 - |\langle\psi(\Delta t)|\psi(\xi)\rangle|^2\right]\right\}. \tag{2}$$

Note that γ is an arbitrary real constant that, for convenience, can be set equal to $\gamma = 2$. Moreover, $d^2(\xi)$ is the squared Fubini-Study distance between $|\psi(\Delta t)\rangle$ and $|\psi(\xi)\rangle$. Performing a Taylor series expansion in Δt and keeping terms up to the fourth order, it is found in Ref. [7] that

$$d_{\min}^2 = \kappa_{\text{LT}}\frac{\gamma^2}{4\hbar^2}(\Delta t)^4 + O(\Delta t^4). \tag{3}$$

The subscript "LT" means Laba and Tkachuk. The quantity κ_{LT} in Eq. (3) is the so-called curvature coefficient introduced by Laba and Tkachuk in Ref. [7] and is given by,

$$\kappa_{\text{LT}} \overset{\text{def}}{=} \langle(\Delta H)^4\rangle - \langle(\Delta H)^2\rangle^2, \tag{4}$$

where $\Delta H \overset{\text{def}}{=} H - \langle H\rangle$ with $\langle H\rangle$ being the expectation value of the constant Hamiltonian H. For completeness, we emphasize that it is possible to define a unitless curvature coefficient $\bar{\kappa}_{\text{LT}} \overset{\text{def}}{=} \kappa_{\text{LT}}/\langle(\Delta H)^2\rangle^2$, that is

$$\bar{\kappa}_{\text{LT}} \overset{\text{def}}{=} \frac{\langle(\Delta H)^4\rangle - \langle(\Delta H)^2\rangle^2}{\langle(\Delta H)^2\rangle^2}. \tag{5}$$

Finally, to offer an alternative geometric interpretation of the unitless curvature coefficient $\bar{\kappa}_{\text{LT}}$, Laba and Tkachuk use a classical analogy. Indeed, any classical trajectory in physical space between two neighboring points can be approximated with a circular trajectory between the two neighboring points. From simple trigonometric arguments, it can be shown that the circle has a radius $R_{\text{classical}}$ that satisfies

$$\frac{1}{R_{\text{classical}}} \overset{d \ll 1}{\approx} \frac{2d}{(s/2)^2}. \tag{6}$$

Recall that the curvature of a circle is the reciprocal of its radius. Note that d in Eq. (6) is the distance between the middle point of an arc and the cord joining the two neighboring points. The quantity s, instead, denotes the length of the circular curve connecting the two points. In the quantum setting, one replaces d in Eq. (6) with $d_{\min}$ in Eq. (3) and, in addition, s in Eq. (6) with $s_{\text{geo}} = 2v\Delta t$ where $v \overset{\text{def}}{=} (\gamma/\hbar)\sqrt{\langle(\Delta H)^2\rangle}$ is the speed of quantum evolution. Then, from Eqs. (3) and (6), one arrives at the conclusion that $\bar{\kappa}_{\text{LT}}$ can be regarded as a quantum analogue of $1/R_{\text{classical}}^2$ (i.e., the squared curvature in a classical setting).

Having discussed the concept of curvature coefficient proposed in Ref. [7], we discuss in the next subsection the notion of torsion coefficient of a quantum evolution.

B. Torsion

In Ref. [7], Laba and Tkachuk propose a concept of torsion coefficient for a Schrödinger quantum-mechanical evolution specified by a time-independent Hamiltonian H. The torsion coefficient quantifies how much the evolving state vector $|\psi(t)\rangle = e^{-(i/\hbar)\mathrm{H}t}|\psi(0)\rangle$ with $0 \leq t \leq t_f$ deviates from the plane of evolution Π at a given time. This plane Π, in turn, is a two-dimensional subspace spanned by two neighboring linearly independent unit state vectors $\{|\psi(0)\rangle, |\psi(\Delta t)\rangle\}$ with $0 \leq \Delta t \leq t_f$ that belong to the plane Π. Observe that $|\psi(0)\rangle$ and $|\psi(\Delta t)\rangle$ are not orthogonal and, in general, $\langle\psi(0)|\psi(\Delta t)\rangle = ae^{i\alpha} \neq 0$ with $a, \alpha \in \mathbb{R}$. From the set $\{|\psi(0)\rangle, |\psi(\Delta t)\rangle\}$, Laba and Tkachuk construct a set of orthonormal vectors $\{|\phi_1\rangle, |\phi_2\rangle\}$ and use it to define an orthogonal projection operator $\mathrm{P}_\Pi \overset{\text{def}}{=} |\phi_1\rangle\langle\phi_1| + |\phi_2\rangle\langle\phi_2|$ onto the plane Π. Then, the magnitude of the deviation of $|\psi(t)\rangle$ from the plane Π is characterized by the scalar quantity $1 - p_\Pi$ with $p_\Pi \overset{\text{def}}{=} \langle\psi(\Delta t + \Delta t')|\mathrm{P}_\Pi|\psi(\Delta t + \Delta t')\rangle$, $\Delta t' \geq 0$, and $0 \leq \Delta t + \Delta t' \leq t_f$. Given the definition of P_Π, note that $p_\Pi = |\langle\phi_1|\psi(\Delta t + \Delta t')\rangle|^2 + |\langle\phi_2|\psi(\Delta t + \Delta t')\rangle|^2$. Therefore, when $p_\Pi = 1$, there is no deviation from the plane of evolution since the three vectors $|\phi_1\rangle$, $|\phi_2\rangle$, and $|\psi(\Delta t + \Delta t')\rangle$ are on the same plane. Therefore, in this case, the torsion coefficient is expected to vanish. More specifically, Laba and Tkachuk introduce the torsion coefficient τ_{LT} in an approximate setting where they Taylor expand $1 - p_\Pi$ up to the fourth order in Δt and $\Delta t'$. Assuming without loss of generality that $\Delta t = \Delta t'$, it is reported in Ref. [7] that

$$1 - p_\Pi = \tau_{\mathrm{LT}}\frac{\Delta t^4}{\hbar^4} + O\left(\Delta t^4\right), \tag{7}$$

where τ_{LT} is a constant coefficient that is independent from Δt and $\Delta t'$ and is given by,

$$\tau_{\mathrm{LT}} \overset{\text{def}}{=} \left\langle(\Delta\mathrm{H})^4\right\rangle - \left\langle(\Delta\mathrm{H})^2\right\rangle^2 - \frac{\left\langle(\Delta\mathrm{H})^3\right\rangle^2}{\left\langle(\Delta\mathrm{H})^2\right\rangle} = \kappa_{LT} - \frac{\langle(\Delta\mathrm{H})^3\rangle^2}{\langle(\Delta\mathrm{H})^2\rangle}. \tag{8}$$

Recall that $\Delta\mathrm{H} \overset{\text{def}}{=} \mathrm{H} - \langle\mathrm{H}\rangle$ with $\langle\mathrm{H}\rangle$ denoting the expectation value of the time-independent Hamiltonian H. For completeness, we remark that it is possible to introduce a unitless torsion coefficient $\bar{\tau}_{\mathrm{LT}} \overset{\text{def}}{=} \tau_{\mathrm{LT}}/\left\langle(\Delta\mathrm{H})^2\right\rangle^2$, that is

$$\bar{\tau}_{\mathrm{LT}} \overset{\text{def}}{=} \frac{\left\langle(\Delta\mathrm{H})^4\right\rangle - \left\langle(\Delta\mathrm{H})^2\right\rangle^2}{\left\langle(\Delta\mathrm{H})^2\right\rangle^2} - \frac{\left\langle(\Delta\mathrm{H})^3\right\rangle^2}{\left\langle(\Delta\mathrm{H})^2\right\rangle^3} = \bar{\kappa}_{LT} - \frac{\langle(\Delta\mathrm{H})^3\rangle^2}{\langle(\Delta\mathrm{H})^2\rangle^3}. \tag{9}$$

Finally, to provide an additional geometric interpretation of the torsion coefficient τ_{LT} in Eq. (8), Laba and Tkachuk show that the scalar quantity $1 - p_\Pi$ happens to be proportional to the squared distance of $|\psi(\Delta t + \Delta t')\rangle$ to the plane Π. Therefore, they conclude that $1 - p_\Pi$ has a clear geometrical interpretation and is a suitable indicator of the presence of torsion during the quantum-mechanical evolution.

Having discussed this relevant background material, in the next section we present some preliminary material on the classical Frenet-Serret apparatus. This, in turn, will inspire our own newly proposed measures of curvature and torsion of a quantum curve.

III. THE CLASSICAL FRENET-SERRET APPARATUS

In this section, in preparation of our newly proposed theoretical construct in Sec. IV, we recall the basic ingredients of a classical Frenet-Serret apparatus with special focus on the concepts of bending and twisting as captured by the curvature and the torsion of a curve in three-dimensional Euclidean space.

A. Essentials

We limit our presentation here to unit speed regular curves in $\mathbb{R}^3$. In this context, the so-called Frenet-Serret apparatus is the main tool to study curves since it completely determines the geometry of the curve. This apparatus consists of three unit vector fields along the curve and two scalar-valued functions. The three vector fields are the tangent vector field $\hat{T}$, the principal normal vector field $\hat{N}$, and the binormal vector field $\hat{B}$. The two scalar-valued functions, instead, are given by the curvature κ_{FS} and the torsion τ_{FS}. The subscript "FS" means Frenet and Serret. The set $\left\{\hat{T}, \hat{N}, \hat{B}\right\}$ is known as the Frenet-Serret frame. It is a very convenient set of three orthonormal vectors that reflects the geometry of the curve and, thus, can be used to fully characterize the geometric properties of a curve in

$\mathbb{R}^3$. Although the Frenet-Serret apparatus can be applied to non-unit speed curves as well, we focus on unit speed curves here. In this latter case, it is possible to show that three vectors specifying the Frenet-Serret frame satisfy the so-called Frenet-Serret equations given by [2]

$$
\begin{pmatrix} \hat{T}' \\ \hat{N}' \\ \hat{B}' \end{pmatrix} = \begin{pmatrix} 0 & \kappa_{\mathrm{FS}} & 0 \\ -\kappa_{\mathrm{FS}} & 0 & \tau_{\mathrm{FS}} \\ 0 & -\tau_{\mathrm{FS}} & 0 \end{pmatrix} \begin{pmatrix} \hat{T} \\ \hat{N} \\ \hat{B} \end{pmatrix}. \tag{10}
$$

The relations in Eq. (10) describe the dynamics of $\left\{ \hat{T}, \hat{N}, \hat{B} \right\}$ in terms of how they move and twist as one walks along the curve. In other words, the Frenet-Serret frame is a classical example of a "moving" frame. The prime in Eq. (10) denotes differentiation with respect the parameter chosen to parametrize the curve, i.e., the arc length s along the curve defined as,

$$
s \stackrel{\text{def}}{=} \int_0^s \left\| \frac{d\vec{\gamma}}{dt} \right\| dt, \tag{11}
$$

with $\vec{\gamma} : (a, b) \rightarrow \mathbb{R}^3$ being a unit speed regular curve with $\|d\vec{\gamma}/dt\| = 1$. Note that $d\vec{\gamma}/dt$ is the velocity vector field along $\vec{\gamma}$. The tangent vector field $\hat{T}(t)$, instead, is the unit vector in the direction of the velocity vector and is defined as $\hat{T}(t) \stackrel{\text{def}}{=} (d\vec{\gamma}/dt) / \|d\vec{\gamma}/dt\|$. For completeness, we observe that curves can be parametrized with parameters other than the arc length s and, in addition, the satisfaction of the regularity condition of the curve requires $d\vec{\gamma}/dt \neq 0$. For a more general discussion on the geometry of curves in $\mathbb{R}^3$ extended to irregular and/or non-unit speed curves, we refer to Ref. [2].

Finally, we shall define the vectors $\hat{N}$ and $\hat{B}$ in the following subsections where the focus is on the concepts of curvature and torsion of a curve in $\mathbb{R}^3$.

B. Curvature

It is generally stated that the curvature of a straight line is equal to zero and that of a circle is constant since it assumes the same value at each point along the curve. These statements suggest that the notion of curvature should provide a measure of the bending of a curve. Assuming a unit-speed regular curve, a reasonable measure of the bending of the curve can be specified by the rate of change $\hat{T}'(s)$ of the tangent vector field $\hat{T}(s)$ with respect to the arc length s. Indeed, the curvature $\kappa_{\mathrm{FS}}(s)$ of a unit-speed regular curve $\vec{\gamma}(s)$ is defined as

$$
\kappa_{\mathrm{FS}}(s) \stackrel{\text{def}}{=} \left\| \hat{T}'(s) \right\|. \tag{12}
$$

Note that, in general, κ_{FS} is non-constant and depends on s. Furthermore, observe that κ_{FS} equals 0 and $1/R$ for a straight line and a circle of radius R, respectively. To better understand the significance of κ_{FS} in Eq. (12) and in preparation of the introduction of the concept of torsion, it is convenient to define at this point the vectors $\hat{N}$ and $\hat{B}$. The principal normal vector field $\hat{N}$ to a unit-speed curve $\vec{\gamma}(s)$ is given by $\hat{N}(s) \stackrel{\text{def}}{=} \hat{T}'(s)/\kappa_{\mathrm{FS}}$ with $\hat{T}(s) \perp \hat{N}(s)$ since $\left\| \hat{T}(s) \right\|^2 = 1$. Then, the binormal vector $\hat{B}(s)$ is defined as the cross product between $\hat{T}(s)$ and $\hat{N}(s)$, $\hat{B}(s) \stackrel{\text{def}}{=} \hat{T}(s) \times \hat{N}(s)$. We are now ready to introduce the torsion τ_{FS} in the next subsection.

C. Torsion

The torsion τ_{FS} of a unit-speed curve $\vec{\gamma}(s)$ is formally defined as,

$$
\tau_{\mathrm{FS}}(s) \stackrel{\text{def}}{=} -\hat{B}'(s) \cdot \hat{N}(s). \tag{13}
$$

From a geometric standpoint, τ_{FS} measures how far the curve $\vec{\gamma}(s)$ is from lying in the osculating plane spanned by the orthonormal vectors $\hat{T}(s)$ and $\hat{N}(s)$. In particular, if a curve lies in a plane at all times, $\tau_{\mathrm{FS}} = 0$ and the plane is the osculating plane. When $\tau_{\mathrm{FS}} \neq 0$, τ_{FS} quantifies the twisting of the curve out of the osculating plane. Furthermore, this twisting does not need to be constant as one walks on the curve. Unlike the curvature κ_{FS}, the torsion τ_{FS} can be both positive and negative. Its sign has a clear geometric meaning. It is positive (or, negative) when the curve twists toward (or, toward the opposite) the side $\hat{B}(s)$ points to as s increases.

In the next section, taking inspiration from what we presented in Sec. III, we propose our definitions of curvature and torsion coefficients of a quantum curve. Remarkably, we recover the curvature and torsion coefficients as presented in Sec. II as originally proposed by Laba and Tkachuk in Ref. [7].

IV. A QUANTUM VERSION OF THE FRENET-SERRET APPARATUS

In this section, we propose a quantum version of the classical Frenet-Serret apparatus. In particular, we propose novel measures of bending and twisting of a quantum curve traced out by a parallel-transported pure quantum state that evolves under the action of a time-independent (Hermitian) Hamiltonian operator.

A. Parallel-transported unit state vectors: $\{|\Psi\rangle\}$

We begin by introducing the parallel-transported unit state vectors $\{|\Psi\rangle\}$ with $\langle\Psi|\Psi\rangle = 1$ and $\left\langle\Psi\middle|\dot{\Psi}\right\rangle = 0$. Consider the normalized state vector $|\psi(t)\rangle$ with $\langle\psi(t)|\psi(t)\rangle = 1$ that satisfies the Schrödinger evolution equation,

$$i\hbar\partial_t|\psi(t)\rangle = \mathrm{H}(t)|\psi(t)\rangle. \tag{14}$$

In what follows, the Hamiltonian $\mathrm{H}(t)$ in Eq. (14) is assumed to be constant in time, i.e., $\mathrm{H}(t) = \mathrm{H}$ for any $t \geq 0$. Observe that $\left|\dot{\psi}(t)\right\rangle \overset{\text{def}}{=} \partial_t|\psi(t)\rangle = -(i/\hbar)\mathrm{H}|\psi(t)\rangle$ is not orthogonal to $|\psi(t)\rangle$ since $\left\langle\psi(t)\middle|\dot{\psi}(t)\right\rangle = -(i/\hbar)\langle\psi(t)|\mathrm{H}|\psi(t)\rangle \neq 0$, in general. Note that $\langle\psi(t)|\mathrm{H}|\psi(t)\rangle$ is time-independent since $\langle\psi(t)|\mathrm{H}|\psi(t)\rangle = \langle\psi(0)|e^{iHt/\hbar}He^{-iHt/\hbar}|\psi(0)\rangle = \langle\psi(0)|\mathrm{H}|\psi(0)\rangle = E =$ constant. Let us define $|\Psi(t)\rangle \overset{\text{def}}{=} e^{i\beta(t)}|\psi(t)\rangle$ with

$$\beta(t) \overset{\text{def}}{=} \frac{1}{\hbar}\int_0^t\langle\psi(t')|\mathrm{H}|\psi(t')\rangle\,dt'. \tag{15}$$

In our case, $\beta(t) = \frac{E}{\hbar}t$ and $|\Psi(t)\rangle = e^{i\frac{E}{\hbar}t}|\psi(t)\rangle$, that is, $|\psi(t)\rangle = e^{-i\frac{E}{\hbar}t}|\Psi(t)\rangle$. By construction, we have $\left\langle\Psi(t)\middle|\dot{\Psi}(t)\right\rangle = 0$ and $|\Psi(t)\rangle$ satisfies the Schrödinger evolution equation

$$i\hbar\partial_t|\Psi(t)\rangle = \Delta\mathrm{H}|\Psi(t)\rangle. \tag{16}$$

In Eq. (16), $\Delta\mathrm{H} \overset{\text{def}}{=} \mathrm{H} - \langle\mathrm{H}\rangle$, with $\langle\mathrm{H}\rangle$ and $\Delta\mathrm{H}$ being time-independent quantities when H is assumed to be time-independent. Having introduced the state vector $|\Psi(t)\rangle$, we are ready to introduce the unit tangent vector in the next subsection.

B. Unit tangent vectors: $\{|T\rangle\}$

In this subsection, we introduce the unit tangent vectors $\{|T\rangle\}$ such that $\langle T|T\rangle = 1$ and $\langle\Psi|T\rangle = 0$. To begin, let us consider the time derivative of the normalized state vector $|\Psi(t)\rangle$, $\left|\bar{T}(t)\right\rangle \overset{\text{def}}{=} \partial_t|\Psi(t)\rangle$. Note that we use the upper bar symbol, like the one in $\left|\bar{T}(t)\right\rangle$, to indicate unnormalized vectors. Using Eq. (16), we have

$$\left|\bar{T}(t)\right\rangle = \partial_t|\Psi(t)\rangle = -\frac{i}{\hbar}\Delta\mathrm{H}|\Psi(t)\rangle. \tag{17}$$

Note that $\left|\bar{T}(t)\right\rangle$ is orthogonal to $|\Psi(t)\rangle$, $\left\langle\Psi(t)\middle|\bar{T}(t)\right\rangle = 0$, since $\langle\psi(t)|\Delta\mathrm{H}|\psi(t)\rangle = 0$. However, $\left|\bar{T}(t)\right\rangle$ is not normalized to one since

$$\left\langle\bar{T}(t)\middle|\bar{T}(t)\right\rangle = -\left(\frac{i}{\hbar}\right)^2\left\langle\Psi(t)\middle|(\Delta\mathrm{H})^2\middle|\Psi(t)\right\rangle = \frac{\left\langle(\Delta\mathrm{H})^2\right\rangle}{\hbar^2} \overset{\text{def}}{=} v^2. \tag{18}$$

The quantity v in Eq. (18) is constant in time and can be used to define the arc length s given by

$$s \overset{\text{def}}{=} \int_0^t v\,dt = vt. \tag{19}$$

For completeness, note that $[t]_{\text{MKSA}} = \sec$, $[v]_{\text{MKSA}} = \sec^{-1}$, and $[s]_{\text{MKSA}}$ is adimensional (i.e., unitless). MKSA denotes meters, kilograms, seconds, and amperes within the International System of Units. From Eq. (19), the relation between t-derivatives and s-derivatives is given by $\partial_s = (1/v)\partial_t$. Using s-derivatives, we can introduce a properly normalized tangent vector $|T(s)\rangle$ defined as

$$|T(s)\rangle \overset{\text{def}}{=} \partial_s |\Psi(s)\rangle \equiv |\Psi'(s)\rangle \equiv -i\Delta h |\Psi(s)\rangle, \tag{20}$$

where $|\Psi(s)\rangle \overset{\text{def}}{=} |\Psi(t(s))\rangle$. Observe that $|T(s)\rangle = -i\Delta h |\Psi(s)\rangle$, where the unitless operator Δh is defined as $\Delta h \overset{\text{def}}{=} \Delta \text{H}/(\hbar v)$. By construction, $|T(s)\rangle$ in Eq. (20) is such that $\langle T(s)|T(s)\rangle = 1$. In addition, it can be rewritten as $|T(s)\rangle = \text{P}^{(\Psi)}|\Psi'(s)\rangle = |\Psi'(s)\rangle$, with $\text{P}^{(\Psi)} \overset{\text{def}}{=} \text{I} - |\Psi\rangle\langle\Psi|$ being a Hermitian projector onto states orthogonal to the unit state vector $|\Psi\rangle$ such that $\text{P}^{(\Psi)}\text{P}^{(\Psi)} = \text{P}^{(\Psi)}$ and $\left(\text{P}^{(\Psi)}\right)^\dagger = \text{P}^{(\Psi)}$. For completeness, using this definition of the tangent vector in terms of the projector operator $\text{P}^{(\Psi)}$, we get $\langle T(s)|T(s)\rangle = \left\langle (\Delta \text{H})^2 \right\rangle / \left(\hbar^2 v^2\right) = 1$ since $v^2 \overset{\text{def}}{=} \left\langle (\Delta \text{H})^2 \right\rangle / \hbar^2$. Lastly, notice that $|T(s)\rangle$ is orthogonal to $|\Psi(s)\rangle$. Indeed, using Eq. (20), we have $\langle \Psi(s)|T(s)\rangle = -i\langle \Psi(s)|\Delta h|\Psi(s)\rangle = -i\langle \Delta h \rangle = 0$ since $\Delta h \overset{\text{def}}{=} \Delta \text{H}/(\hbar v) = \Delta \text{H}/\sqrt{\langle \Delta \text{H}^2 \rangle}$ with $\langle \Delta \text{H} \rangle = 0$. In summary, $\{|\Psi(s)\rangle, |T(s)\rangle\}$ is a pair of orthonormal state vectors. Moreover, $|T(s)\rangle$ is the projection of $|\Psi'(s)\rangle$ normal to $|\Psi(s)\rangle$ and specifies the so-called covariant derivative of $|\Psi(s)\rangle$, $|T(s)\rangle = |\text{D}\Psi(s)\rangle \overset{\text{def}}{=} \text{P}^{(\Psi)}|\Psi'(s)\rangle$. The covariant derivative operator D is defined as $\text{D} \overset{\text{def}}{=} \text{P}^{(\Psi)}(d/ds)$ and represents the projection onto a state perpendicular to $|\Psi(s)\rangle$ of the ordinary derivative d/ds with s being the arc length [15, 20, 21]. The set of vectors $\{|\Psi(s)\rangle, |T(s)\rangle\}$ can be viewed as spanning the instantaneous "osculating" plane that contains the quantum curve traced out by the state vector $|\Psi(s)\rangle$. This plane will play a key role when introducing the concept of torsion of a quantum evolution. Before doing so, we introduce in the next subsection a concept of curvature for quantum evolutions.

C. Curvature

In our approach, inspired by the classical Frenet-Serret apparatus, we propose that the curvature coefficient κ_{AC}^2 is given by the magnitude squared of the covariant derivative of the tangent vector $|T(s)\rangle$ to the state vector $|\Psi(s)\rangle$,

$$\kappa_{\text{AC}}^2 \overset{\text{def}}{=} \left\langle T'(s) \left| \left(\text{P}^{(\Psi)}\right)^\dagger \text{P}^{(\Psi)} \right| T'(s) \right\rangle, \tag{21}$$

with $\text{D}|T(s)\rangle \overset{\text{def}}{=} \text{P}^{(\Psi)}|T'(s)\rangle$ and $\text{D} \overset{\text{def}}{=} \text{P}^{(\Psi)}\frac{d}{ds} = (\text{I} - |\Psi\rangle\langle\Psi|)\frac{d}{ds}$ [15, 20, 21]. The subscript "AC" means Alsing and Cafaro. Since $|T'(s)\rangle = |\Psi''(s)\rangle$ and $\text{P}^{(\Psi)}|T(s)\rangle = |T(s)\rangle$, κ_{AC}^2 in Eq. (21) can be regarded as specified by the second covariant derivative $\text{D}^2|\Psi(s)\rangle$ of the state vector $|\Psi(s)\rangle$ (i.e., a form of acceleration vector) and can be recast as

$$\kappa_{\text{AC}}^2 \overset{\text{def}}{=} \|\text{D}|T(s)\rangle\|^2 = \left\|\text{D}^2 |\Psi(s)\rangle\right\|^2. \tag{22}$$

Note that while κ_{AC}^2 in Eq. (22) is the squared magnitude of the second covariant derivative of the state vector $|\Psi(s)\rangle$ that traces out the quantum Schrödinger trajectory, κ_{FS} in Eq. (12) is the magnitude of the second derivative of the vector position $\vec{r}(s)$ that traces out the unit-speed curve $\vec{\gamma}(s)$ in the FS apparatus. Thus, our proposed curvature coefficient κ_{AC}^2 can be regarded as a quantum analogue of κ_{FS}^2. To find an explicit expression of κ_{AC}^2 in Eq. ((21), we use Eq. (20) to obtain $\text{P}^{(\Psi)}|T'(s)\rangle = -\left[(\Delta h)^2 - \left\langle (\Delta h)^2 \right\rangle\right]|\Psi(s)\rangle$. Indeed, dropping the "$s$" in $|\Psi(s)\rangle$ and $|T(s)\rangle$, we have

$$
\begin{aligned}
\text{P}^{(\Psi)}|T'\rangle &= \text{P}^{(\Psi)}|\partial_s T\rangle \\
&= \text{P}^{(\Psi)}\partial_s\left(-i\Delta h|\Psi\rangle\right) \\
&= -i\text{P}^{(\Psi)}\left(\Delta h|\partial_s\Psi\rangle\right) \\
&= -i\text{P}^{(\Psi)}\left(\Delta h|T\rangle\right) \\
&= -i\text{P}^{(\Psi)}\left(-i(\Delta h)^2|\Psi\rangle\right) \\
&= -\left[\text{I} - |\Psi\rangle\langle\Psi|\right]\left[(\Delta h)^2|\Psi\rangle\right] \\
&= -\left[(\Delta h)^2|\Psi\rangle - \left\langle\Psi\left|(\Delta h)^2\right|\Psi\right\rangle|\Psi\rangle\right] \\
&= -\left[(\Delta h)^2 - \left\langle(\Delta h)^2\right\rangle\right]|\Psi\rangle.
\end{aligned} \tag{23}
$$

From Eq. (23), we finally get an expression of the curvature coefficient κ_{AC}^2 in terms of expectation values of powers of the adimensional operator Δh,

$$\kappa_{\mathrm{AC}}^2 = \left\langle (\Delta h)^4 \right\rangle - \left\langle (\Delta h)^2 \right\rangle^2 = \left\langle (\Delta h)^4 \right\rangle - 1, \tag{24}$$

where we have used $\langle (\Delta h)^2 \rangle = \langle \left(\Delta H / \sqrt{\langle (\Delta H)^2 \rangle} \right)^2 \rangle = 1$. Interestingly, we note that κ_{AC}^2 in Eq. (24) coincides with the unitless curvature coefficient introduced by Laba and Tkachuk given by $\bar{\kappa}_{\mathrm{LT}} \stackrel{\text{def}}{=} \kappa_{\mathrm{LT}} / \langle (\Delta H)^2 \rangle^2$ in Eq. (5) with κ_{LT} given in Eq. (4) once we recall that $\Delta h = \Delta H / \sqrt{\langle (\Delta H)^2 \rangle}$. We are now ready to introduce our proposal for a concept of torsion for a quantum evolution.

D. Torsion

We begin by recalling that in the classical Frenet-Serret apparatus, the definition of the torsion coefficient requires the introduction of the binormal vector field $\hat{B}(s)$ that is orthogonal to the instantaneous osculating plane spanned by the other two orthonormal vectors $\hat{T}(s)$ and $\hat{N}(s)$. In our quantum framework, the instantaneous motion of the curve belongs to the plane spanned by the orthonormal state vectors $|\Psi(s)\rangle$ and $|T(s)\rangle$. This plane can be viewed as the quantum analogue of the osculating plane that appears in the Frenet-Serret apparatus. Furthermore, it corresponds to the plane spanned by the state vectors $|\psi(t)\rangle$ and $|\psi(t + \Delta t)\rangle$ in the quantum Laba-Tkachuk framework once one recognizes that the linear approximation of $|\psi(t + \Delta t)\rangle$ is given by $|\psi(t)\rangle + |\dot{\psi}(t)\rangle \Delta t + O(\Delta t^2)$ with $|\dot{\psi}(t)\rangle = |\partial_t \psi(t)\rangle$ with $\partial_t \stackrel{\text{def}}{=} \partial / \partial t$. However, we need to identify a suitable quantum analogue of $\hat{B}(s)$. We start by recalling that while $\{|\Psi(s)\rangle, |T(s)\rangle\}$ forms an orthonormal set of state vectors and $\mathrm{P}^{(\Psi)} |T'(s)\rangle$ is orthogonal to $|\Psi(s)\rangle$, we have two issues. First, $\mathrm{P}^{(\Psi)} |T'(s)\rangle$ and $|T(s)\rangle$ are not orthogonal since $\langle T(s) | \mathrm{P}^{(\Psi)} | T'(s)\rangle = -i \left\langle (\Delta h)^3 \right\rangle \neq 0$. Interestingly, as we shall see better later, $\left\langle (\Delta h)^3 \right\rangle$ corresponds to the so-called skewness coefficient in statistical mathematics [22–24]. Second, $\mathrm{P}^{(\Psi)} |T'(s)\rangle$ is not properly normalized to one. This latter matter is a minor concern. To address the first issue, we propose to consider the (not normalized) state vector $|\bar{N}(s)\rangle$ defined as,

$$\left| \bar{N}(s) \right\rangle \stackrel{\text{def}}{=} \mathrm{P}^{(T)} \mathrm{P}^{(\Psi)} |T'(s)\rangle, \tag{25}$$

that is, $\left| \bar{N}(s) \right\rangle \stackrel{\text{def}}{=} \mathrm{P}^{(T)} \mathrm{D} |T(s)\rangle$. By construction, $\left| \bar{N}(s) \right\rangle$ in Eq. (25) is orthogonal to both $|\Psi(s)\rangle$ and $|T(s)\rangle$. Clearly, one can construct a properly normalized vector $|N(s)\rangle$ from $\left| \bar{N}(s) \right\rangle$ given by $|N(s)\rangle \stackrel{\text{def}}{=} \left| \bar{N}(s) \right\rangle / \left\| \bar{N}(s) \right\|$ so that $\{|\Psi(s)\rangle, |T(s)\rangle, |N(s)\rangle\}$ forms a useful set of orthonormal state vectors. Interestingly, $\{|\Psi(s)\rangle, |T(s)\rangle, |N(s)\rangle\}$ can be regarded as the outcome of an ordinary Gram-Schmidt orthonormalization procedure applied to the input set of (linearly independent) vectors given by $\{|\Psi(s)\rangle, |\Psi'(s)\rangle, |\Psi''(s)\rangle\}$ or, equivalently, $\{|\Psi(s)\rangle, \mathrm{D}|\Psi(s)\rangle, \mathrm{D}^2 |\Psi(s)\rangle\}$. We show in Fig. 1 a graphical depiction of the Frenet-Serret frame $\left\{ \hat{T}, \hat{N}, \hat{B} \right\}$ for the vector spaces along a curve in three-dimensional Euclidean space $\mathbb{R}^3$ along with a pictorial representation of our proposed quantum frame $\{|\Psi(s)\rangle, |T(s)\rangle, |N(s)\rangle\}$ for the three-dimensional subspaces along a curve on a generalized Bloch sphere. At this point, we can finally propose of notion of torsion coefficient τ_{AC}^2 given by,

$$\tau_{\mathrm{AC}}^2 \stackrel{\text{def}}{=} \left\| |\bar{N}(s)\rangle \right\|^2 = \left\langle T'(s) \left| \left(\mathrm{P}^{(T)} \mathrm{P}^{(\Psi)} \right)^\dagger \mathrm{P}^{(T)} \mathrm{P}^{(\Psi)} \right| T'(s) \right\rangle = \left\langle T'(s) \left| \mathrm{P}^{(\Psi)} \mathrm{P}^{(T)} \mathrm{P}^{(\Psi)} \right| T'(s) \right\rangle. \tag{26}$$

In terms of the state vector $\left| \bar{N}(s) \right\rangle \stackrel{\text{def}}{=} \mathrm{P}^{(T)} \mathrm{P}^{(\Psi)} |T'(s)\rangle$, τ_{AC}^2 can be recast as

$$\tau_{\mathrm{AC}}^2 \stackrel{\text{def}}{=} \left\langle \bar{N}(s) | \bar{N}(s) \right\rangle = \left\| \mathrm{P}^{(T)} \mathrm{D} |T(s)\rangle \right\|^2. \tag{27}$$

Observe that since $\left| \bar{N}(s) \right\rangle$ in Eq. (25) can be recast as $\mathrm{P}^{(T)} \mathrm{D}^2 |\Psi(s)\rangle$ with $\mathrm{D}^2 |\Psi(s)\rangle = \mathrm{P}^{(\Psi)} |T'(s)\rangle$, $\left| \bar{N}(s) \right\rangle$ can be viewed as the projection of the second covariant derivative $\mathrm{D}^2 |\Psi(s)\rangle$ of the state vector $|\Psi(s)\rangle$ onto a state orthogonal to $|T(s)\rangle$. Therefore, by construction using $P^T P^\Psi$ we have that $\left| \bar{N}(s) \right\rangle$ is a vector that is orthogonal to the "osculating" plane spanned by $|\Psi(s)\rangle$ and $|T(s)\rangle$. Therefore, by construction, τ_{AC}^2 measures how far the quantum curve traced out by $|\Psi(s)\rangle$ is lifting off from the instantaneous "osculating" plane spanned by the orthonormal set
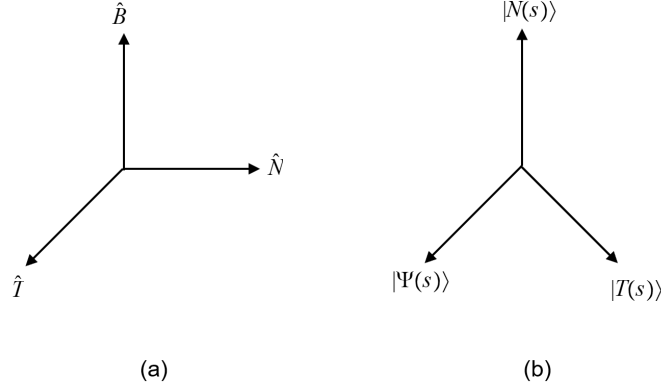
FIG. 1: (a) Graphical depiction of the Frenet-Serret frame $\left\{\hat{T},\ \hat{N},\ \hat{B}\right\}$ for the vector spaces along a curve in three-dimensional Euclidean space $\mathbb{R}^3$. (b) Pictorial representation of our proposed quantum frame $\{|\Psi(s)\rangle,\ |T(s)\rangle,\ |N(s)\rangle\}$ for the three-dimensional subspaces along a curve on a generalized Bloch sphere $\mathbb{C}P^{N-1} = \mathcal{S}^{2N-1}/\mathcal{S}^1$ where $\mathcal{S}^k$ denotes a k-sphere and N is the dimensionality of the complex Hilbert space. For $N=2$, the quantum curve is on the Bloch sphere $\mathbb{C}P^1 = \mathcal{S}^3/\mathcal{S}^1 = \mathcal{S}^2$ and $|N(s)\rangle$ is identically zero. A set of three orthonormal vectors is sufficient to define the first two generalized curvature functions, i.e. the curvature and the torsion coefficients.

of vectors $|\Psi(s)\rangle$ and $|T(s)\rangle$. Thus, τ_{AC}^2 is a measure of the twisting of the Schrödinger type quantum-mechanical evolution under investigation and is, by construction, a quantum analogue of τ_{LT}^2 with τ_{LT} in Eq. (13) introduced in the classical FS apparatus. To find an explicit expression of τ_{AC}^2 in Eq. (26), we first substitute Eq. (25) into Eq. (26). Then, recalling that $\langle \Psi(s)|\Delta h|\Psi(s)\rangle = 0$, we get

$$\tau_{\mathrm{AC}}^2 = \left\langle \Psi(s) \left| \left[(\Delta h)^2 - \langle (\Delta h)^2 \rangle - \Delta h \langle (\Delta h)^3 \rangle \right]^2 \right| \Psi(s) \right\rangle \geq 0, \tag{28}$$

where the last inequality follows since the argument of the expectation value is the square of a Hermitian operator. Then, expanding Eq. (28) and noting that $\langle \Delta h \rangle = 0$ and $\left\langle (\Delta h)^2 \right\rangle = 1$, τ_{AC}^2 in Eq. (28) reduces to

$$\tau_{\mathrm{AC}}^2 = \left\langle (\Delta h)^4 \right\rangle - \left\langle (\Delta h)^3 \right\rangle^2 - 1 = \kappa_{AC}^2 - \left\langle (\Delta h)^3 \right\rangle^2. \tag{29}$$

Interestingly, we note that τ_{AC}^2 in Eq. (29) coincides with the unitless torsion coefficient introduced by Laba and Tkachuk given by $\bar{\tau}_{\mathrm{LT}} \overset{\mathrm{def}}{=} \tau_{\mathrm{LT}}/\left\langle (\Delta H)^2 \right\rangle^2$ with τ_{LT} in Eq. (8) once we observe that $\Delta h = \Delta \mathrm{H}/\sqrt{\langle (\Delta \mathrm{H})^2 \rangle}$. Finally, combining Eqs. (24) and (29), we also recover the same constraint relation as in the Laba-Tkachuk framework, i.e., $\kappa_{\mathrm{AC}}^2 = \tau_{\mathrm{AC}}^2 + \left\langle (\Delta h)^3 \right\rangle^2$.

In the next section, we present several points of discussion that emerge from our newly proposed concepts of curvature and torsion of a quantum evolution.

V. DISCUSSION

We begin this section with a discussion on the statistical interpretation of the curvature and torsion coefficients in Eqs. (21) and (26), respectively. We then show the utility of rewriting the expressions of these two coefficients in terms of the Bloch vector for two-level systems. We proceed by elaborating on several challenges that can arise in higher-dimensional Hilbert spaces with quantum evolutions governed by nonstationary Hamiltonians. We finally conclude with a comparison between our proposed quantum apparatus and the classical Frenet-Serret one.

A. Statistical interpretation of curvature and torsion

In mathematical statistics, the skewness and the kurtosis are two quantities used to characterize the shape of a probability distribution. The skewness involves the third moment of the distribution and is a measure of the

"asymmetry" of the probability distribution. It is defined as a unitless coefficient α_3 given by [22, 23],

$$\alpha_3 \overset{\text{def}}{=} \sqrt{\frac{m_3^2}{m_2^3}} = \frac{m_3}{m_2^{3/2}}, \tag{30}$$

where m_r is the rth central moment,

$$m_r \overset{\text{def}}{=} \frac{1}{n} \sum_{i=1}^{n} (x_i - \bar{x})^r, \tag{31}$$

and $\bar{x}$ is the arithmetic mean of n real numbers x_i with $1 \le i \le n$. Therefore, m_3 and m_2 in Eq. (30) are the third moment and the variance of the data set. The kurtosis, instead, involves the fourth moment of the distribution and is a measure of the "tailedness" of the probability distribution (i.e., a quantifier of how often outliers occur). It is defined as the unitless coefficient α_4 defined as [22, 23],

$$\alpha_4 \overset{\text{def}}{=} \frac{m_4}{m_2^2}. \tag{32}$$

A well-known inequality in mathematical statistics is the so-called Pearson inequality [24],

$$\alpha_4 \ge \alpha_3^2 + 1. \tag{33}$$

For later use, we employ Eqs. (30) and (32) to recast the Pearson inequality $\alpha_4 - 1 - \alpha_3^2 \ge 0$ as

$$\frac{m_4 - m_2^2}{m_2^2} - \frac{m_3^2}{m_2^3} \ge 0. \tag{34}$$

Interestingly, our proposed curvature and torsion coefficients κ_{AC}^2 and τ_{AC}^2, respectively, have a neat mathematical statistics interpretation. Indeed, we point the attention to the following correspondences,

$$\kappa_{\text{AC}}^2 = \frac{\left\langle (\Delta \text{H})^4 \right\rangle - \left\langle (\Delta \text{H})^2 \right\rangle^2}{\left\langle (\Delta \text{H})^2 \right\rangle^2} \longleftrightarrow \alpha_4 - 1 = \frac{m_4 - m_2^2}{m_2^2}, \tag{35}$$

and,

$$\tau_{\text{AC}}^2 = \frac{\left\langle (\Delta \text{H})^4 \right\rangle - \left\langle (\Delta \text{H})^2 \right\rangle^2}{\left\langle (\Delta \text{H})^2 \right\rangle^2} - \frac{\left\langle (\Delta \text{H})^3 \right\rangle^2}{\left\langle (\Delta \text{H})^2 \right\rangle^3} \longleftrightarrow \alpha_4 - 1 - \alpha_3^2 = \frac{m_4 - m_2^2}{m_2^2} - \frac{m_3^2}{m_2^3}. \tag{36}$$

From Eqs. (35) and (36) we note that the curvature and the torsion coefficients can be regarded in terms of statistically meaningful quantum quantities, $\kappa_{\text{AC}}^2 \longleftrightarrow \alpha_4 - 1$ and $\tau_{\text{AC}}^2 \longleftrightarrow \alpha_4 - 1 - \alpha_3^2$. In particular, the difference $\kappa_{\text{AC}}^2 - \tau_{\text{AC}}^2$ between the curvature and the torsion coefficient is captured by the square of the skewness coefficient, $\alpha_3^2 = \kappa_{\text{AC}}^2 - \tau_{\text{AC}}^2$. This last inequality can be interpreted as follows. Let us convey to denote a quantum state "symmetric" if $\left\langle (\Delta \text{H})^3 \right\rangle$ is vanishing under the quantum evolution governed by the stationary Hamiltonian H. Then, the curvature and the torsion of a quantum curve traced out by a symmetric state are identical. The symmetry encoded in the quantum state for a given Hamiltonian manifests itself in the vanishing third moment $\left\langle (\Delta \text{H})^3 \right\rangle$, whose presence signifies the existence of asymmetric quantum behavior of statistical nature. Finally, the validity of the Pearson inequality in Eq. (34) is a straightforward consequence of the positivity of τ_{AC}^2 in Eq. (36).

B.   Curvature, torsion, and the Bloch vector for 2-level systems

Although our geometric approach is formally valid for arbitrary d-level quantum systems with $d \ge 2$, we focus here on two-level systems. Consider a physical system specified by the density operator $\rho(t) \overset{\text{def}}{=} [\text{I} + \mathbf{a}(t) \cdot \vec{\sigma}]/2$ that evolves under the traceless stationary Hamiltonian $\text{H} \overset{\text{def}}{=} \mathbf{m} \cdot \vec{\sigma}$. The vectors $\mathbf{a}$ and $\mathbf{m}$ denote the Bloch vector and the magnetic

vector, respectively. For the case of pure states considered here, $\mathbf{a} \cdot \mathbf{a} = 1$ is a unit vector on the Bloch sphere. Recall that an arbitrary qubit observable $Q = q_0 \mathrm{I} + \mathbf{q} \cdot \vec{\sigma}$ with $q_0 \in \mathbb{R}$ and $\mathbf{q} \in \mathbb{R}^3$ has a corresponding expectation value given by $\langle Q \rangle_\rho = q_0 + \mathbf{a} \cdot \mathbf{q}$. In what follows, we would like to express the curvature and the torsion coefficients κ_{AC}^2 and τ_{AC}^2, respectively, in terms of the vectors $\mathbf{a}$ and $\mathbf{m}$.

Recall that,

$$\kappa_{\mathrm{AC}}^2 \overset{\mathrm{def}}{=} \left\langle (\Delta h)^4 \right\rangle - \left\langle (\Delta h)^2 \right\rangle^2 = \frac{\left\langle (\Delta \mathrm{H})^4 \right\rangle - \left\langle (\Delta \mathrm{H})^2 \right\rangle^2}{\left\langle (\Delta \mathrm{H})^2 \right\rangle^2}. \tag{37}$$

By brute force expansion and using the fact that $\mathrm{H}^2 = \mathbf{m}^2 \mathrm{I}$, we get

$$\begin{aligned}
\left\langle (\Delta \mathrm{H})^4 \right\rangle &= \left\langle \mathrm{H}^4 \right\rangle - 4 \left\langle \mathrm{H}^3 \right\rangle \langle \mathrm{H} \rangle + 6 \left\langle \mathrm{H}^2 \right\rangle \langle \mathrm{H} \rangle^2 - 3 \langle \mathrm{H} \rangle^4 \\
&= \left\langle \mathrm{H}^4 \right\rangle - 4 \left\langle \mathrm{H}^2 \right\rangle \langle \mathrm{H} \rangle^2 + 6 \left\langle \mathrm{H}^2 \right\rangle \langle \mathrm{H} \rangle^2 - 3 \langle \mathrm{H} \rangle^4 \\
&= \left\langle \mathrm{H}^4 \right\rangle + 2 \left\langle \mathrm{H}^2 \right\rangle \langle \mathrm{H} \rangle^2 - 3 \langle \mathrm{H} \rangle^4,
\end{aligned} \tag{38}$$

where we have used $H^3 = \mathbf{m}^2 H = \left\langle H^2 \right\rangle H$ and in addition,

$$\left\langle (\Delta \mathrm{H})^2 \right\rangle^2 = \left\langle \mathrm{H}^2 \right\rangle^2 + \langle \mathrm{H} \rangle^4 - 2 \left\langle \mathrm{H}^2 \right\rangle \langle \mathrm{H} \rangle^2. \tag{39}$$

Combining Eqs. (38) and (39) and using the fact $\left\langle \mathrm{H}^4 \right\rangle = \left\langle \mathrm{H}^2 \right\rangle^2 = \mathbf{m}^4$, we arrive at

$$\begin{aligned}
\left\langle (\Delta \mathrm{H})^4 \right\rangle - \left\langle (\Delta \mathrm{H})^2 \right\rangle^2 &= \left(\left\langle \mathrm{H}^4 \right\rangle + 2 \left\langle \mathrm{H}^2 \right\rangle \langle \mathrm{H} \rangle^2 - 3 \langle \mathrm{H} \rangle^4 \right) - \left(\left\langle \mathrm{H}^2 \right\rangle^2 + \langle \mathrm{H} \rangle^4 - 2 \left\langle \mathrm{H}^2 \right\rangle \langle \mathrm{H} \rangle^2 \right) \\
&= \left(\left\langle \mathrm{H}^4 \right\rangle - \left\langle \mathrm{H}^2 \right\rangle^2 \right) + 4 \left\langle \mathrm{H}^2 \right\rangle \langle \mathrm{H} \rangle^2 - 4 \langle \mathrm{H} \rangle^4 \\
&= 4 \langle \mathrm{H} \rangle^2 \left(\left\langle \mathrm{H}^2 \right\rangle - \langle \mathrm{H} \rangle^2 \right) \\
&= 4 \langle \mathrm{H} \rangle^2 \left\langle (\Delta \mathrm{H})^2 \right\rangle,
\end{aligned} \tag{40}$$

that is,

$$\left\langle (\Delta \mathrm{H})^4 \right\rangle - \left\langle (\Delta \mathrm{H})^2 \right\rangle^2 = 4 \langle \mathrm{H} \rangle^2 \left\langle (\Delta \mathrm{H})^2 \right\rangle. \tag{41}$$

Using Eq. (41), κ_{AC}^2 in Eq. (37) becomes

$$\kappa_{\mathrm{AC}}^2 = 4 \frac{\langle \mathrm{H} \rangle^2}{\left\langle (\Delta \mathrm{H})^2 \right\rangle}. \tag{42}$$

Then, observing that $\langle \mathrm{H} \rangle^2 = (\mathbf{a} \cdot \mathbf{m})^2$ and $\left\langle (\Delta \mathrm{H})^2 \right\rangle = \mathbf{m}^2 - (\mathbf{a} \cdot \mathbf{m})^2$, we finally arrive at the expression for $\kappa_{\mathrm{AC}}^2 (\mathbf{a}, \mathbf{m})$,

$$\kappa_{\mathrm{AC}}^2 (\mathbf{a}, \mathbf{m}) = 4 \frac{(\mathbf{a} \cdot \mathbf{m})^2}{\mathbf{m}^2 - (\mathbf{a} \cdot \mathbf{m})^2}. \tag{43}$$

Remember that the torsion coefficient τ_{AC}^2 is given by,

$$\tau_{\mathrm{AC}}^2 = \left\langle (\Delta h)^4 \right\rangle - \left\langle (\Delta h)^2 \right\rangle^2 - \left\langle (\Delta h)^3 \right\rangle^2 = \frac{\left\langle (\Delta \mathrm{H})^4 \right\rangle - \left\langle (\Delta \mathrm{H})^2 \right\rangle^2}{\left\langle (\Delta \mathrm{H})^2 \right\rangle^2} - \frac{\left\langle (\Delta \mathrm{H})^3 \right\rangle^2}{\left\langle (\Delta \mathrm{H})^2 \right\rangle^3} = \kappa_{\mathrm{AC}}^2 - \frac{\left\langle (\Delta \mathrm{H})^3 \right\rangle^2}{\left\langle (\Delta \mathrm{H})^2 \right\rangle^3}. \tag{44}$$

Observe that $\left\langle (\Delta \mathrm{H})^3 \right\rangle$ can be recast as,

$$\left\langle (\Delta \mathrm{H})^3 \right\rangle = \left\langle \mathrm{H}^3 \right\rangle - 3 \left\langle \mathrm{H}^2 \right\rangle \langle \mathrm{H} \rangle + 2 \langle \mathrm{H} \rangle^3. \tag{45}$$

Then, noting that $\mathrm{H}^2 = \mathbf{m}^2\mathrm{I}$ and $\mathrm{H}^3 = \mathbf{m}^2\left(\mathbf{m}\cdot\vec{\sigma}\right)$, $\left\langle\left(\Delta\mathrm{H}\right)^3\right\rangle$ in Eq. (45) reduces to

$$\left\langle\left(\Delta\mathrm{H}\right)^3\right\rangle = -2\left\langle\mathrm{H}\right\rangle\left\langle\left(\Delta\mathrm{H}\right)^2\right\rangle. \tag{46}$$

For later use, we emphasize that in terms of the vectors $\mathbf{a}$ and $\mathbf{m}$, $\left\langle\left(\Delta\mathrm{H}\right)^3\right\rangle$ in Eq. (46) can be rewritten as $-2\left(\mathbf{a}\cdot\mathbf{m}\right)\left[\mathbf{m}^2 - \left(\mathbf{a}\cdot\mathbf{m}\right)^2\right]$. We reiterate that Eq. (46) has been obtained when the single-qubit quantum state evolves under a traceless stationary Hamiltonian of the form $\mathrm{H} = \mathbf{m}\cdot\vec{\sigma}$. Finally, employing Eqs. (42), (44), and (46), we obtain

$$\tau_{\mathrm{AC}}^2\left(\mathbf{a},\,\mathbf{m}\right) = 0. \tag{47}$$

Interestingly, the vanishing of the torsion coefficient in the case of motion on a Bloch sphere can be explained in terms of the projector formalism as well. Recall that τ_{AC}^2 is formally defined as the norm squared of the vector $\left|\bar{N}\left(s\right)\right\rangle \overset{\mathrm{def}}{=} \mathrm{P}^{(T)}\mathrm{P}^{(\Psi)}\left|T'(s)\right\rangle$. Note that $\mathrm{I} = \mathrm{I}_{\mathcal{H}_2^1} \overset{\mathrm{def}}{=} \left|\Psi\right\rangle\left|\Psi\right| + \left|T\right\rangle\left|T\right|$ with $\dim_{\mathbb{C}}\mathcal{H}_2^1 = 2$. Clearly, $\mathcal{H}_2^1$ denotes here the Hilbert space of single-qubit ($k = 1$, superscript) quantum states of dimension $d = 2$ (subscript). Furthermore, given that $\mathrm{P}^{(\Psi)} \overset{\mathrm{def}}{=} \mathrm{I} - \left|\Psi\right\rangle\left\langle\Psi\right|$, $\mathrm{P}^{(T)} \overset{\mathrm{def}}{=} \mathrm{I} - \left|T\right\rangle\left\langle T\right|$, and $\mathrm{P}^{(\Psi)}\mathrm{P}^{(T)} = \mathrm{P}^{(T)}\mathrm{P}^{(\Psi)} = \mathcal{O}$ (with $\mathcal{O}$ being the null operator) since $\left|\Psi\right\rangle$ and $\left|T\right\rangle$ are orthonormal, we have

$$\begin{aligned}
\mathrm{P}^{(T)}\mathrm{P}^{(\Psi)} &= \left(\mathrm{I} - \left|T\right\rangle\left\langle T\right|\right)\left(\mathrm{I} - \left|\Psi\right\rangle\left\langle\Psi\right|\right) \\
&= \mathrm{I} - \left|\Psi\right\rangle\left\langle\Psi\right| - \left|T\right\rangle\left\langle T\right| \\
&= \mathrm{I} - \mathrm{I} \\
&= \mathcal{O}.
\end{aligned} \tag{48}$$

Observe that for higher-dimensional systems, $\mathrm{P}^{(\Psi)}\mathrm{P}^{(T)}$ is not necessarily the null operator $\mathcal{O}$ since since $\left\{\left|\Psi\right\rangle,\,\left|T\right\rangle\right\}$ is not a complete set (in other words, the resolution of the identity cannot be obtained by simply using $\left|\Psi\right\rangle$ and $\left|T\right\rangle$, in general higher-dimensional scenarios).

As a final remark, we observe that geodesic motion occurs when $\kappa_{\mathrm{AC}}^2\left(\mathbf{a},\,\mathbf{m}\right) = 0$, i.e., when $\mathbf{a}\perp\mathbf{m}$ from Eq. (43). In this case, the kurtosis assumes its minimum value of one (since $\alpha_4 = 1 \leftrightarrow \left\langle\left(\Delta\mathrm{h}\right)^4\right\rangle = 1$) and the skewness vanishes (since $\alpha_3 = 0 \leftrightarrow \left\langle\left(\Delta\mathrm{h}\right)^3\right\rangle = 0$). Therefore, we conclude that geodesic quantum motion specified by a stationary Hamiltonian on the Bloch sphere occurs, from a statistical standpoint, with minimal sharpness together with maximal symmetry.

C. Extension to higher-dimensional state spaces

In our current investigation, the expressions for κ_{AC}^2 and τ_{AC}^2 are formally valid for arbitrary d-level quantum systems evolving under stationary Hamiltonians. In our illustrative examples, however, we shall limit the use of the notion of Bloch vectors to Bloch spheres for 2-level systems. Interestingly, the concept of Bloch vector can be formally extended to 4-level two-qubit systems [25] and to arbitrary d-dimensional quantum systems with $d > 2$ (i.e., qudits) [26–28]. For single-qubit systems, the usefulness of the Bloch vector formalism is twofold. First, the unitary time evolution of a single-qubit quantum state can be captured as an orbit on the Bloch spheres. The orbit gives a clear visualization of the quantum mechanical time evolution. Second, the Bloch vector has real components that can be expressed as expectation values of experimentally measurable observables specified by Hermitian operators (i.e., the Pauli operators in the single-qubit scenario). When moving from single-qubit quantum systems to higher dimensional systems, the physical interpretation of the Bloch vector preserves its usefulness. Unfortunately, its geometric visualization is not as clear as in the 2-level systems. Indeed, bizarre properties of quantum theory emerge in higher-dimensional systems, including the simplest but non-trivial case represented by 3-level systems (i.e., qutrits) [28]. These bizarre quantum features make it difficult to reveal the geometry of multidimensional quantum systems [29, 30]. A significant departure between single-qubit systems and higher-dimensional quantum systems is the following. For qubits, any point on the Bloch sphere or inside the Bloch ball corresponds to a physical state (i.e., a pure and a mixed quantum state, respectively). For d-dimensional qudit systems, instead, not every point on the "Bloch sphere" in dimensions $d^2 - 1$ corresponds to a physical state. Although it is possible to construct a unique Bloch vector for any physical state, not every Bloch vector corresponds to a quantum state. In particular, there is in higher-dimensions the emergence of Bloch vectors that correspond to unphysical states specified by density matrices with negative eigenvalues (though

still of trace one, [28]). Thus, one must also enforce the non-trivial condition of the positivity of the corresponding density matrix for these states [16]. For an interesting discussion on Bloch vector representations of single-qubit systems, single-qutrit systems, and two-qubit systems in terms of Pauli, Gell-Mann, and Dirac matrices, respectively, we refer to Ref. [31]. We shall attempt to extend our geometric intuition beyond the simplest quantum systems together with considering the physical significance of the concepts of curvature and torsion coefficients in relation to generalized "Bloch spheres" in forthcoming scientific endeavors.

D.   Extension to nonstationary quantum evolutions

We have limited here our investigation to stationary Hamiltonian evolutions and time-independent expressions for the coefficients κ_{AC}^2 and τ_{AC}^2. In the stationary scenario, the exact calculation of the dynamical trajectory traced out by the source state does not present any significant problem. Although our geometric formalism yielding time-dependent expressions for κ_{AC}^2 and τ_{AC}^2 can be formally extended to the time-dependent setting [32], we expect that finding analytical expressions for the dynamical trajectories traced out by source states evolving under arbitrary time-dependent Hamiltonians will be generally rather challenging. Indeed, it is known that it is very difficult to find exact analytical solutions to the time-dependent Schrödinger equation even for two-level quantum systems. The first examples of analytically solvable two-state time-dependent problems were presented by Landau-Zener in Refs. [33, 34] and Rabi in Refs. [35, 36]. The effort of finding analytical solutions has been very intense throughout the years. For a partial list of relevant works on two-state time-dependent problems that have appeared in the last ten years, we suggest [37–41] and references therein. Finally, for a relatively recent work on finding exact analytical solutions for specific classes of non-stationary Hamiltonians for d-level quantum systems (i.e., qudits), we suggest Ref. [42]. We shall further investigate these issues in Ref. [32].

E.   Comparison with the Frenet-Serret apparatus

As previously mentioned, our proposed geometric construction of curvature and torsion coefficients for quantum evolutions takes its original inspiration from considering curves in three-dimensional Euclidean space framed in terms of the Frenet-Serret frame [2, 43]. However, it is important to emphasize that the classical Frenet-Serret apparatus formalism can be extended to study curves in the higher-dimensional Euclidean space $\mathbb{R}^n$ [44] and, more interestingly, there is a freedom in constructing frames and corresponding apparatuses when studying the local geometry of curves in $\mathbb{R}^n$ [45]. The Frenet-Serret "moving frame" is just one geometrically nice orthonormal basis for the vector spaces along a curve, where the basis vectors move and twist as one moves along the curve. Clearly, there is more than one way to frame a curve in $\mathbb{R}^3$. For instance, the canonical orthonormal basis of $\mathbb{R}^3$, $\{\hat{e}_1,\, \hat{e}_2,\, \hat{e}_3\}$ with $\hat{e}_1 \overset{\text{def}}{=} (1,\, 0,\, 0)$, $\hat{e}_2 \overset{\text{def}}{=} (0,\, 1,\, 0)$, and $\hat{e}_3 \overset{\text{def}}{=} (0,\, 0,\, 1)$ is a legitimate basis for the vector spaces along a curve. However, $\{\hat{e}_1,\, \hat{e}_2,\, \hat{e}_3\}$ reflects the geometry of $\mathbb{R}^3$ rather than the geometry of the curve. The Frenet-Serret frame, instead, is an intrinsically geometric basis that reflects the geometry of the curve. It has the peculiarity that the frame is adapted to the curve, that is, its members are either tangent to or perpendicular to the curve. We recall that moving frames are orthonormal basis fields that can be used to express the derivatives of the frame with respect to the curve parameter in terms of the frame itself. Due to orthonormality, the coefficient matrix (also known as, the Cartan matrix) that relates the derivatives of the frame to the frame itself is always skew-symmetric. Therefore, this matrix has three nonzero entries, in general. The Frenet-Serret frame has only two nonzero entries which are specified by two scalar-valued functions (i.e., the curvature κ_{FS} and the torsion τ_{FS} coefficients). As previously mentioned, it is possible to show that there exist other adapted frames which have only two nonzero entries in their Cartan matrices as well [45]. Despite the fact that these alternative frames (constructed, for instance, within the so-called normal development of a curve [45]) yield geometric invariants that do not posses an equally nice geometric interpretation as the one available for the Frenet invariants, they only require 2-times continuously differentiable curves with a nonzero first derivative γ' of the curve γ in $\mathbb{R}^3$. A Frenet-Serret apparatus of a curve γ in $\mathbb{R}^3$, instead, requires 3-times differentiability along with nondegeneracy (i.e., the first and second derivatives of the curve, γ' and γ'', respectively, must be linearly independent).

Unlike what happens in the quantum setting being considered here, the curve is given a priori in the classical Frenet-Serret apparatus. Indeed, the curve is not generated by any Hamiltonian and is not necessarily a solution of any specific differential equation of motion. From the curve, one can construct the set of orthonormal vectors (i.e., the Frenet-Serret frame) from the derivatives of the curve. However, if the curve is a non-unit speed curve which is parametrized by ordinary time rather than the arc length, the curvature and the torsion coefficients can be expressed in terms of more complicated functions of derivatives of the curve up to third order [2]. In general, the classical Frenet-Serret apparatus is built for curves in n-dimensional (real) Euclidean spaces $\mathbb{R}^n$ equipped with

a real inner product. Our proposed quantum apparatus, instead, is formally constructed for curves on generalized "Bloch spheres" $\mathbb{C}P^{N-1} = S^{2N-1}/S^1$. The space $\mathbb{C}P^{N-1}$ can be viewed as the quotient of the unit $(2N-1)$-sphere in the N-dimensional complex space $\mathbb{C}^N$ under the action of $S^1 = U(1)$. For instance, in the case of the two-dimensional complex Hilbert space for single-qubit quantum states, we consider curves on the usual Bloch sphere. Despite these differences, in analogy to the classical Frenet-Serret apparatus, we propose a quantum apparatus for curves to which is given (in principle, at least) a unit speed parametrization by means of the arc length parameter. Moreover, similarly to the Frenet-Serret frame, our proposed quantum frame is determined by applying the Gram-Schmidt (GS) orthonormalization process. However, while for space curves in $\mathbb{R}^3$, the GS procedure is applied to $\{\gamma'(s), \gamma''(s), \gamma'''(s)\}$, in our case we apply it to the set $\{|\Psi(s)\rangle, |\Psi'(s)\rangle, |\Psi''(s)\rangle\}$. Therefore, in analogy to the above-mentioned alternative frames for curves in $\mathbb{R}^n$, we only require 2-times continuously differentiable quantum curves with a nonvanishing first derivative $|\Psi'(s)\rangle$ of the state vector $|\Psi(s)\rangle$. For clarity, recall that the quantum curve, $s \to |\Psi(s)\rangle$, is the one traced by the state $|\Psi(s)\rangle$. More specifically, in the Frenet-Serret case of a space curve in $\mathbb{R}^3$, we recall that the coefficient matrix $\mathrm{M}^{(\mathrm{FS})}_{\partial_s(\mathrm{Frame}) \to \mathrm{Frame}}$ that expresses the derivatives of the frame with respect to the curve parameter s in terms of the frame itself is given by [2]

$$\mathrm{M}^{(\mathrm{FS})}_{\partial_s(\mathrm{Frame}) \to \mathrm{Frame}} = \begin{pmatrix} 0 & \kappa_{\mathrm{FS}} & 0 \\ -\kappa_{\mathrm{FS}} & 0 & \tau_{\mathrm{FS}} \\ 0 & -\tau_{\mathrm{FS}} & 0 \end{pmatrix}. \tag{49}$$

In our quantum scenario, instead, focusing on the three-dimensional subspace of $\mathbb{C}^N$ spanned by the quantum frame $\{|\Psi(s)\rangle, |T(s)\rangle, |N(s)\rangle\}$, the analog of Eq. (49) is generally given by

$$\mathrm{M}^{(\mathrm{AC})}_{\partial_s(\mathrm{Frame}) \to \mathrm{Frame}} = \begin{pmatrix} 0 & 1 & 0 \\ -1 & i\,\mathrm{Im}(e^{i\phi\langle T|T'\rangle}\sqrt{\kappa_{\mathrm{AC}}^2 - \tau_{\mathrm{AC}}^2}) & e^{i\phi\langle N|T'\rangle}\tau_{\mathrm{AC}} \\ 0 & -e^{-i\phi\langle N|T'\rangle}\tau_{\mathrm{AC}} & i\,\mathrm{Im}(\langle N|N'\rangle) \end{pmatrix}. \tag{50}$$

Note that in Eq. (50) we used the usual exponential representation of a complex number, $z = |z|\,e^{i\phi_z}$ with ϕ_z being the (real) argument of z. In addition, $\tau_{\mathrm{AC}} = |\langle N|T'\rangle|$, $\kappa_{\mathrm{AC}}^2 = |\langle T|T'\rangle|^2 + |\langle N|T'\rangle|^2$, and $|\langle T|T'\rangle| = \sqrt{\kappa_{\mathrm{AC}}^2 - \tau_{\mathrm{AC}}^2}$. Finally, observe that $\mathrm{Re}\left[\mathrm{M}^{(\mathrm{FS})}_{\partial_s(\mathrm{Frame}) \to \mathrm{Frame}}\right]$ is skew-symmetric and, more generally, $\mathrm{M}^{(\mathrm{AC})}_{\partial_s(\mathrm{Frame}) \to \mathrm{Frame}}$ is skew-Hermitian. Essentially, skew-Hermitian matrices are the complex versions of the real skew-symmetric matrices. Moreover, while $\mathrm{M}^{(\mathrm{FS})}_{\partial_s(\mathrm{Frame}) \to \mathrm{Frame}}$ in Eq. (49) has only two nonzero (real) entries, $\mathrm{M}^{(\mathrm{AC})}_{\partial_s(\mathrm{Frame}) \to \mathrm{Frame}}$ in Eq. (50) has generally three nonzero (complex) entries. Finally, although using a different frame as evident from Eqs. (49) and (50), we also propose good measures to quantify the failures of linearity and planarity in terms of suitable curvature κ_{AC} and torsion τ_{AC} coefficients, respectively. For illustrative purposes, we provide an explicit example of the construction of a quantum frame for a quantum curve traced by a two-qubit quantum state on a generalized "Bloch sphere" in $\mathbb{C}^4$ in Appendix A. For clarity, we present in Fig. 2 a sketch of two orthonormal position vectors locating two points on a 2-sphere viewed as the boundary of a 3-ball in R^3 and, in addition, we draw two orthonormal unit Bloch vectors locating two orthogonal quantum states. Finally, before presenting our conclusive remarks in Sec. VII, we show some illustrative examples in the next section.

VI. ILLUSTRATIVE EXAMPLES

We exhibit in this section simple illustrative examples of the behavior of curvature and torsion coefficients in Eqs. (21) and (26), respectively, for quantum evolutions specified by single-qubit and two-qubit time-independent Hamiltonians.

Recall that in classical physics, the force that appears in Newton's second law depends only on the gradient of the potential and a constant additive term is physically irrelevant. Potential differences, instead, have physical significance. Analogously, in the quantum setting, there is no absolute energy and the physics of $\mathrm{H}_1 \overset{\mathrm{def}}{=} m_0 \mathrm{I} + \mathbf{m} \cdot \vec{\sigma}$ and $\mathrm{H}_2 \overset{\mathrm{def}}{=} \mathbf{m} \cdot \vec{\sigma}$ for a single qubit is the same. In particular, although $\langle \mathrm{H}_1 \rangle = m_0 \neq 0$ and $\langle \mathrm{H}_2 \rangle = 0$, we have that $\Delta\mathrm{H}_1 \overset{\mathrm{def}}{=} \mathrm{H}_1 - \langle \mathrm{H}_1 \rangle$ equals $\Delta\mathrm{H}_2 \overset{\mathrm{def}}{=} \mathrm{H}_2 - \langle \mathrm{H}_2 \rangle$ with $\Delta\mathrm{H}_2 = \mathbf{m} \cdot \vec{\sigma}$. Therefore, the curvature coefficients that emerge from the Hamiltonians H_1 and H_2 are identical. Interestingly, the expectation value of a traceless Hamiltonian such as H_2 can be different from zero. When this happens, we have a nonvanishing curvature of the quantum evolution. For a traceless Hamiltonian to generate geodesic motion, its expectation value must be zero. Indeed, the most general single-qubit geodesic evolution defined by a traceless time-independent Hamiltonian is given by $\mathrm{H} = E_1 |E_1\rangle\langle E_1| + E_2 |E_2\rangle\langle E_2|$, with $\mathrm{H}|E_i\rangle = E_i |E_i\rangle$
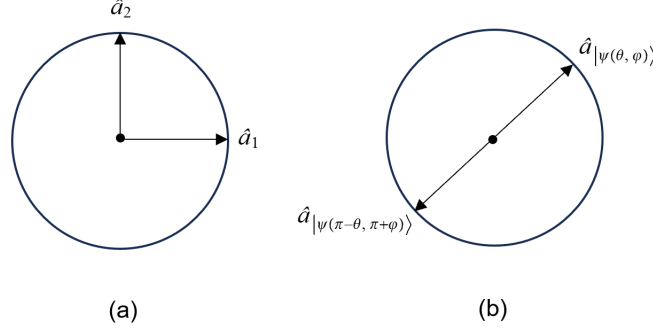
FIG. 2: (a) Sketch of two orthonormal position vectors locating two points on a 2-sphere viewed as the boundary of a 3-ball in $\mathbb{R}^3$. (b) Drawing of two orthonormal Bloch vectors locating two orthogonal quantum states. Antipodal states on the Bloch sphere $|\psi(\theta, \varphi)\rangle \overset{\text{def}}{=} \cos(\theta/2)|0\rangle + e^{i\varphi}\sin(\theta/2)|1\rangle$ and $|\psi(\pi - \theta, \pi + \varphi)\rangle$ with Bloch vectors $\hat{a}_{|\psi(\theta,\varphi)\rangle} = (\sin(\theta)\cos(\varphi), \sin(\theta)\sin(\varphi), \cos(\theta))$ and $\hat{a}_{|\psi(\pi-\theta,\pi+\varphi)\rangle} = -\hat{a}_{|\psi(\theta,\varphi)\rangle}$, respectively, are orthogonal. The Bloch sphere is not to be regarded as the usual sphere in three-dimensional coordinate space $\mathbb{R}^3$. In particular, the latter can be viewed as the "double cover" of the former.

for $1 \leq i \leq 2$ and $E_2 = -E_1 = E$, acting on a source state $|A\rangle = (1/\sqrt{2})\left[|E_1\rangle + e^{i\phi}|E_2\rangle\right]$ with $\phi \in \mathbb{R}$ [46]. In this case, the evolved state is given by

$$|\psi(t)\rangle = \frac{e^{-i(E_1/\hbar)t}}{\sqrt{2}}\left[|E_1\rangle + e^{i\phi}e^{-i[(E_2-E_1)/\hbar]t}|E_2\rangle\right]. \tag{51}$$

A straightforward calculation shows that $\langle H\rangle = 0$ and, thus, κ_{AC}^2 vanishes for the quantum curve traced out by the state $|\psi(t)\rangle$ in Eq. (51). However, it is possible to have a non-traceless Hamiltonian that exhibits geodesic motion even if its expectation value is different from zero. Finally, the torsion coefficient τ_{AC}^2 vanishes for any traceless time-independent single-qubit Hamiltonian of the form H$= \mathbf{m}\cdot\vec{\sigma}$, regardless of the expectation value of the Hamiltonian.

1. Zero curvature and zero torsion: single qubit

Consider the spin precession that specifies the evolution of a spin-1/2 particle (an electron, for instance) with magnetic moment $e\hbar/(2m_e c)$ (with $e \leq 0$, for an electron) subjected to a stationary magnetic field $\mathbf{B}$. Clearly, c is the speed of light and m_e denotes the mass of the electron. Then, the Hamiltonian of the system becomes H$\overset{\text{def}}{=} \mathbf{m}\cdot\vec{\sigma}$ with $\mathbf{m} \overset{\text{def}}{=} |e|\mathbf{B}/(2m_e c)$. In this first example, let us assume $\mathbf{m} = (0, 0, m)$ with $m \overset{\text{def}}{=} |e| B_z/(2m_e c)$. The quantum trajectory is assumed to be traced out by the state $|\psi(t)\rangle = U(t)|\psi(0)\rangle$ with $U(t) \overset{\text{def}}{=} \exp\left[-(i/\hbar)\text{H}t\right]$ being the unitary evolution operator and $|\psi(0)\rangle$ the chosen initial state vector. We assume that the unit states $|\psi(t)\rangle$ with $t_A \leq t \leq t_B$ are given by

$$|\psi(t)\rangle = \frac{e^{-i(m/\hbar)t}}{\sqrt{2}}\left[|0\rangle + e^{i(2m/\hbar)t}|1\rangle\right]. \tag{52}$$

These states in Eq. (52) can be regarded as states on the Bloch sphere that can be parametrized in spherical coordinates as $|\psi(\theta, \varphi)\rangle = \cos(\theta/2)|0\rangle + e^{i\varphi}\sin(\theta/2)|1\rangle$ with a corresponding Bloch vector $\mathbf{a} = (\sin(\theta)\cos(\varphi), \sin(\theta)\sin(\varphi), \cos(\theta))$. The initial and terminal states are given by $|A\rangle \overset{\text{def}}{=} |\psi(\theta_A, \varphi_A)\rangle$ and $|B\rangle \overset{\text{def}}{=} |\psi(\theta_B, \varphi_B)\rangle$, respectively. From Eq. (52), it is clear that we choose $(\theta_A, \varphi_A) \overset{\text{def}}{=} (\pi/2, 0)$, $(\theta_B, \varphi_B) \overset{\text{def}}{=} (\pi/2, \pi/2)$, and $0 \leq t \leq \hbar\pi/4m$. Therefore, the initial and final states $|A\rangle = [|0\rangle + |1\rangle]/\sqrt{2}$ and $|B\rangle = [|0\rangle + i|1\rangle]/\sqrt{2}$ are specified by Bloch vectors $\mathbf{a}_{\text{initial}} = (1, 0, 0)$ and $\mathbf{a}_{\text{final}} = (0, 1, 0)$, respectively. A simple calculation yields $\kappa_{\text{AC}}^2 = 4(\mathbf{a}\cdot\mathbf{m})^2/[\mathbf{m}^2 - (\mathbf{a}\cdot\mathbf{m})^2] = 0$ since the traceless Hamiltonian H$= m\sigma_z$ has a vanishing expectation value, $\langle H\rangle = \mathbf{a}\cdot\mathbf{m} = 0$ with $\mathbf{a} = \mathbf{a}_{\text{initial}}$. This, in turn, is a consequence of the fact that the Bloch vector $\mathbf{a}_{\text{initial}}$ of the source state is orthogonal to the applied magnetic field $\mathbf{B} \overset{\text{def}}{=} (2m_e c/|e|)\mathbf{m}$.
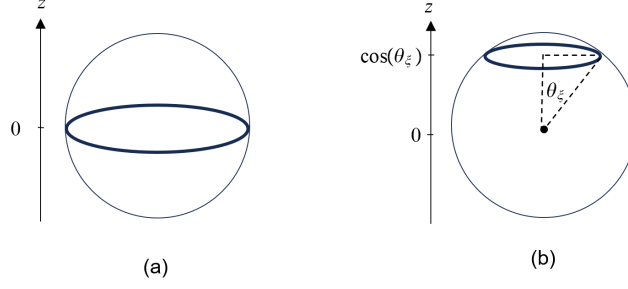
FIG. 3: (a) The tick solid line is a graphical depiction of the circular path on the Bloch sphere traced out by evolving the initial state $|\psi(0)\rangle \overset{\text{def}}{=} (1/\sqrt{2})|0\rangle + (1/\sqrt{2})|1\rangle$ under the Hamiltonian $\text{H} \overset{\text{def}}{=} \hbar\omega_0\sigma_z$. In this case, $|\Psi(s)\rangle = (e^{-is}|0\rangle + e^{is}|1\rangle)/\sqrt{2}$, $|T(s)\rangle = \left(-ie^{-is}|0\rangle + ie^{is}|1\rangle\right)/\sqrt{2}$, $\hat{a}_{|\Psi(s)\rangle} = (\cos(2s), \sin(2s), 0)$, and $\hat{a}_{|T(s)\rangle} = -\hat{a}_{|\Psi(s)\rangle}$, with $s \overset{\text{def}}{=} \omega_0 t$. In this case, $\kappa_{\text{AC}}^2 = 0$. (b) The tick solid line represents the circular path on the Bloch sphere traced out by evolving the initial state $|\psi(0)\rangle \overset{\text{def}}{=} \cos(\theta_\xi/2)|0\rangle + \sin(\theta_\xi/2)|1\rangle$ under the Hamiltonian $\text{H} \overset{\text{def}}{=} \hbar\omega_0\sigma_z$. Note that case (a) assumes $\theta_\xi = \pi/2$. In case (b), $|\Psi(s)\rangle = \cos(\theta_\xi/2)e^{-i\tan(\theta_\xi/2)s}|0\rangle + \sin(\theta_\xi/2)e^{i\cot(\theta_\xi/2)s}|1\rangle$, $|T(s)\rangle = -i\sin(\theta_\xi/2)e^{-i\tan(\theta_\xi/2)s}|0\rangle + i\cos(\theta_\xi/2)e^{i\cot(\theta_\xi/2)s}|1\rangle$, $\hat{a}_{|\Psi(s)\rangle} = \sin(\theta_\xi)\cos\{[\tan(\theta_\xi/2) + \cot(\theta_\xi/2)]s\}\hat{x} + \sin(\theta_\xi)\sin\{[\tan(\theta_\xi/2) + \cot(\theta_\xi/2)]s\}\hat{y} + \cos(\theta_\xi)\hat{z}$, and $\hat{a}_{|T(s)\rangle} = -\hat{a}_{|\Psi(s)\rangle}$, with $s \overset{\text{def}}{=} \omega_0 t$. Unlike case (a), in this case the curvature coefficient is nonzero since $\kappa_{\text{AC}}^2 = 4\left[\cos^2(\theta_\xi)/\sin^2(\theta_\xi)\right] \neq 0$ when $\theta_\xi \neq \pi/2$.

2. Nonzero curvature and zero torsion: single qubit

In analogy to the vanishing curvature case, we consider the quantum evolution under the traceless Hamiltonian $\text{H} \overset{\text{def}}{=} \mathbf{m} \cdot \vec{\sigma}$ where $\mathbf{m} = (0, 0, m)$ with $m \overset{\text{def}}{=} |e|B_z/(2m_ec)$. Again, the quantum trajectory is assumed to be traced out by the state $|\psi(t)\rangle = U(t)|\psi(0)\rangle$ with $U(t) \overset{\text{def}}{=} \exp\left[-(i/\hbar)\text{H}t\right]$ being the unitary evolution operator and $|\psi(0)\rangle$ the chosen initial state vector. Unlike the previous case, we assume now that the unit states $|\psi(t)\rangle$ with $t_A \leq t \leq t_B$ are given by

$$|\psi(t)\rangle = e^{-i(m/\hbar)t}\left[\frac{\sqrt{2+\sqrt{2}}}{2}|0\rangle + e^{i(2m/\hbar)t}\frac{\sqrt{2-\sqrt{2}}}{2}|1\rangle\right]. \tag{53}$$

These states in Eq. (53) can be regarded as state on the Bloch sphere that can be parametrized as $|\psi(\theta, \varphi)\rangle = \cos(\theta/2)|0\rangle + e^{i\varphi}\sin(\theta/2)|1\rangle$ with corresponding Bloch vector $\mathbf{a} = (\sin(\theta)\cos(\varphi), \sin(\theta)\sin(\varphi), \cos(\theta))$. The initial (source) and final (target) states are $|A\rangle \overset{\text{def}}{=} |\psi(\theta_A, \varphi_A)\rangle$ and $|B\rangle \overset{\text{def}}{=} |\psi(\theta_B, \varphi_B)\rangle$, respectively. From Eq. (53), it is clear that we choose $(\theta_A, \varphi_A) \overset{\text{def}}{=} (\pi/4, 0)$, $(\theta_B, \varphi_B) \overset{\text{def}}{=} (\pi/4, \pi/2)$, and $0 \leq t \leq \hbar\pi/4m$. Therefore, the initial and final states $|A\rangle = (\sqrt{2+\sqrt{2}}/2)|0\rangle + (\sqrt{2-\sqrt{2}}/2)|1\rangle$ and $|B\rangle = (\sqrt{2+\sqrt{2}}/2)|0\rangle + i(\sqrt{2-\sqrt{2}}/2)|1\rangle$ are specified by Bloch vectors $\mathbf{a}_{\text{initial}} = (1/\sqrt{2}, 0, 1/\sqrt{2})$ and $\mathbf{a}_{\text{final}} = (0, 1/\sqrt{2}, 1/\sqrt{2})$, respectively. A simple calculation yields $\kappa_{\text{AC}}^2 = 4(\mathbf{a} \cdot \mathbf{m})^2/[\mathbf{m}^2 - (\mathbf{a} \cdot \mathbf{m})^2] = 4 \neq 0$ since the traceless Hamiltonian $\text{H} = m\sigma_z$ has a nonvanishing expectation value, $\langle \text{H} \rangle = \mathbf{a} \cdot \mathbf{m} = m/\sqrt{2} \neq 0$ with $\mathbf{a} = \mathbf{a}_{\text{initial}}$. This, in turn, is a consequence of the fact that the Bloch vector $\mathbf{a}_{\text{initial}}$ of the source state is not orthogonal to the applied magnetic field $\mathbf{B} \overset{\text{def}}{=} (2m_ec/|e|)\mathbf{m}$.

3. Link between curvature and geodesic efficiency: single qubit

We emphasize that the temporal evolutions in Eqs. (52) and (53) can be regarded as special cases of the evolution given by

$$|\psi(t)\rangle = e^{-i(h/\hbar)t}\left[\xi|0\rangle + e^{i(2h/\hbar)t}\sqrt{1-\xi^2}|1\rangle\right], \tag{54}$$

with $\xi = \cos(\theta_\xi/2) \in [0,1]$ and $\theta_\xi \in [0, \pi]$ such that $\mathbf{a} = \left(2\xi\sqrt{1-\xi^2}, 0, 2\xi^2 - 1\right)$, $\cos(\theta_\xi) = 2\xi^2 - 1$, and $\sin(\theta_\xi) = 2\xi\sqrt{1-\xi^2}$. The vanishing and nonvanishing curvature cases previously discussed correspond to $\xi = 1/\sqrt{2}$ and

$\xi = \sqrt{2 + \sqrt{2}}/2$, respectively. In this more general case, the curvature coefficient κ_{AC}^2 is given by

$$\kappa_{\mathrm{AC}}^2 (\xi) = \frac{\left(1 - 2\xi^2\right)^2}{\xi^2 \left(1 - \xi^2\right)} = 4 \frac{\cos^2 (\theta_\xi)}{\sin^2 (\theta_\xi)}. \tag{55}$$

We show in Fig. 3 a graphical depiction of the circular path on the Bloch sphere traced out by evolving the initial states $|\psi(0)\rangle \overset{\text{def}}{=} (1/\sqrt{2}) |0\rangle + (1/\sqrt{2}) |1\rangle$ and $|\psi(0)\rangle \overset{\text{def}}{=} \cos(\theta_\xi/2) |0\rangle + \sin(\theta_\xi/2) |1\rangle$ with $\theta_\xi \neq \pi/2$ under the Hamiltonian $\mathrm{H} \overset{\text{def}}{=} \hbar\omega_0 \sigma_z$. Motivated by the expression of $\kappa_{\mathrm{AC}}^2 (\xi)$ in Eq. (55), we present a discussion on the link between the concept of geodesic curvature in classical differential geometry and our proposed curvature coefficient for quantum evolutions in Appendix B. Clearly, $\kappa_{\mathrm{AC}}^2 (\xi)$ in Eq. (55) assumes its minimum value of zero at $\xi = 1/\sqrt{2} \approx 0.71$ (i.e., polar angle $\theta_\xi = \pi/2 \approx 1.57$). We observe that the local behavior of $\kappa_{\mathrm{AC}}^2 (\xi)$ as a measure of the deviation from geodesic motion is consistent with that exhibited by the so-called geodesic efficiency as introduced in Refs. [14, 47],

$$\eta \overset{\text{def}}{=} 1 - \frac{\Delta s}{s} = \frac{2 \cos^{-1} \left[|\langle A|B\rangle|\right]}{2 \int_{t_A}^{t_B} \frac{\Delta E(t')}{\hbar} dt'}. \tag{56}$$

In Eq. (56), $0 \leq \eta \leq 1$, $\Delta s \overset{\text{def}}{=} s - s_0$, s_0 denotes the distance along the shortest geodesic path that connects the distinct initial $|A\rangle \overset{\text{def}}{=} |\psi(t_A)\rangle$ and final $|B\rangle \overset{\text{def}}{=} |\psi(t_B)\rangle$ states on the projective Hilbert space, $\Delta E(t) \overset{\text{def}}{=} \sqrt{\left\langle \left(\Delta \mathrm{H}(t)\right)^2 \right\rangle}$ and finally, s is the distance along the dynamical trajectory traced out by the state vector $|\psi(t)\rangle$ with $t_A \leq t \leq t_B$. Indeed, from the evolution specified in Eq. (54), the efficiency η in Eq. (56) reduces to

$$\eta(t; \xi) = \frac{\arccos \left(\sqrt{\cos^2 \left(\frac{m}{\hbar} t\right) + \left(2\xi^2 - 1\right)^2 \sin^2 \left(\frac{m}{\hbar} t\right)}\right)}{2\xi \sqrt{1 - \xi^2} \left(\frac{m}{\hbar} t\right)} = \frac{\arccos \left(\sqrt{\cos^2 \left(\frac{m}{\hbar} t\right) + \cos^2 (\theta_\xi) \sin^2 \left(\frac{m}{\hbar} t\right)}\right)}{\sin(\theta_\xi) \left(\frac{m}{\hbar} t\right)}, \tag{57}$$

assuming $t_A = 0$ and $t_B = t$. In particular, taking $t_B = \hbar\pi/4m$ as in the previous two examples, the efficiency $\eta(t; \xi)$ in Eq. (57) reduces to

$$\eta(\xi) = \frac{2}{\pi} \frac{\arccos \left(\sqrt{2\xi^4 - 2\xi^2 + 1}\right)}{\xi \sqrt{1 - \xi^2}} = \frac{4}{\pi} \frac{\arccos \left(\sqrt{\frac{1 + \cos^2(\theta_\xi)}{2}}\right)}{\sin(\theta_\xi)}. \tag{58}$$

As expected, $\eta(\xi) \in [0, 1]$ in Eq. (58) assumes its maximum value of one at $\xi = 1/\sqrt{2} \approx 0.71$ (i.e., polar angle $\theta_\xi = \pi/2 \approx 1.57$) where $\kappa_{\mathrm{AC}}^2 (\xi)$ in Eq. (55) achieves its minimum of zero. In conclusion, we reiterate that the local behavior (for detecting geodesicity) of $\kappa_{\mathrm{AC}}^2 (\xi)$ in Eq. (55) is consistent with that exhibited by $\eta(\xi)$ in Eq. (58). In Fig. 4, we present a visual comparison between the geodesic efficiency and the curvature coefficient for the example discussed here. Moreover, we also show a visualization of a quantum-mechanical realization of the Pearson inequality (i.e., $\alpha_4 \geq \alpha_3^2 + 1$) in mathematical statistics between the kurtosis (α_4) and the skewness (α_3) of a probability distribution function.

4. Nonzero curvature and nonzero torsion: two qubits

As previously mentioned, the torsion coefficient τ_{AC}^2 vanishes for any traceless time-independent single-qubit Hamiltonian of the form $\mathrm{H} = \mathbf{m} \cdot \vec{\sigma}$, regardless of the expectation value of the Hamiltonian. In what follows, we present two examples of nonzero torsion curves traced out by two-qubit quantum states evolving under two-qubit time-independent Hamiltonians. Recall that a general bipartite Hamiltonian H can be written as [48],

$$\mathrm{H} \overset{\text{def}}{=} \mathrm{H}^{(1)} \otimes \mathrm{I}^{(2)} + \mathrm{I}^{(1)} \otimes \mathrm{H}^{(2)} + \sum_{i,j=1}^{3} M_{ij} \Sigma_i^{(1)} \otimes \Sigma_j^{(2)}, \tag{59}$$

where $\{\Sigma_i\}_{1 \leq i \leq 3}$ is a basis for traceless Hermitian operators and $\{M_{ij}\}_{1 \leq i,j \leq 3}$ are coupling coefficients that correspond to the pairwise interaction terms $\left\{\Sigma_i^{(1)} \otimes \Sigma_j^{(2)}\right\}_{1 \leq i,j \leq 3}$. From Eq. (59), the most general purely nonlocal two-qubit
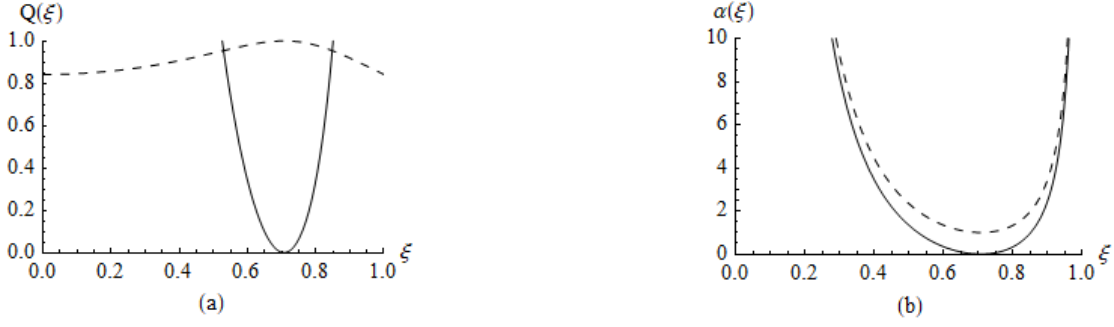
FIG. 4: (a) Plot of the geodesic efficiency $\eta\left(t;\xi\right)\overset{\text{def}}{=}\arccos\left(\sqrt{\cos^2\left(\omega_0 t\right)+\left(2\xi^2-1\right)^2\sin^2\left(\omega_0 t\right)}\right)/\left[2\xi\sqrt{1-\xi^2}\left(\omega_0 t\right)\right]$ $(Q\left(\xi\right)\overset{\text{def}}{=}$ $\eta\left(1;\xi\right)$, black dashed line) and the normalized curvature coefficient $\kappa_{\text{AC}}^2\left(\xi\right)\overset{\text{def}}{=}\left(1-2\xi^2\right)^2/\left[\xi^2\left(1-\xi^2\right)\right]=4\left[\cos^2(\theta_\xi)/\sin^2(\theta_\xi)\right]$ $(Q\left(\xi\right)\overset{\text{def}}{=}\kappa_{\text{AC}}^2\left(\xi\right)$, black solid line) as a function of the parameter $\xi\in[0,1]$ with $\xi\overset{\text{def}}{=}\cos(\theta_\xi/2)$ where θ_ξ is the polar angle such that $0\leq\theta_\xi\leq\pi$. The quantum evolution is assumed to be described by the time-independent Hamiltonian $\text{H}\overset{\text{def}}{=}\hbar\omega_0\sigma_z$ that evolves the initial state $\left|\psi\left(\xi,\varphi\right)\right\rangle\overset{\text{def}}{=}\xi\left|0\right\rangle+e^{i\varphi}\sqrt{1-\xi^2}\left|1\right\rangle$ with $\varphi=0$ (i.e., xz-plane). When plotting the efficiency, we set ω_0 and t equal to one. (b) We exhibit a quantum-mechanical realization of the so-called Pearson inequality (i.e., $\alpha_4\geq\alpha_3^2+1$) in mathematical statistics between the kurtosis (α_4) and the skewness (α_3) of a probability distribution function. We plot the kurtosis $\alpha_4\overset{\text{def}}{=}\left\langle\left(\Delta\text{H}\right)^4\right\rangle/\left\langle\left(\Delta\text{H}\right)^2\right\rangle^2=\left(1-3\xi^2+3\xi^4\right)/\left[\xi^2\left(1-\xi^2\right)\right]$ $(\alpha\left(\xi\right)\overset{\text{def}}{=}\alpha_4\left(\xi\right)$, black dashed line) and the skewness (squared) $\alpha_3^2\overset{\text{def}}{=}\left\langle\left(\Delta\text{H}\right)^3\right\rangle^2/\left\langle\left(\Delta\text{H}\right)^2\right\rangle^3=\left(1-2\xi^2\right)^2/\left[\xi^2\left(1-\xi^2\right)\right]$ $(\alpha\left(\xi\right)\overset{\text{def}}{=}\alpha_3^2\left(\xi\right)$, black solid line) as a function of the parameter $\xi\in[0,1]$ with $\xi\overset{\text{def}}{=}\cos(\theta_\xi/2)$ where θ_ξ is the polar angle such that $0\leq\theta_\xi\leq\pi$. The quantum evolution in (b) is the same as in (a). The geodesic evolution occurs for $\xi=1/\sqrt{2}$. From (a), we note that $\kappa_{\text{AC}}^2\left(1/\sqrt{2}\right)=0$ and $\eta\left(1;1/\sqrt{2}\right)=1$. Finally, we observe from (b) that $\alpha_4\left(1/\sqrt{2}\right)=1$, $\alpha_3^2\left(1/\sqrt{2}\right)=0$, and the Pearson inequality saturates becoming the identity $\alpha_4=\alpha_3^2+1$.

Hamiltonian $\text{H}_{\text{nonlocal}}$ (i.e., $\text{H}_{\text{nonlocal}}\neq\text{H}^{(1)}\otimes\text{I}^{(2)}+\text{I}^{(1)}\otimes\text{H}^{(2)}$) can be written as

$$\text{H}_{\text{nonlocal}}\overset{\text{def}}{=}\sum_{i,j=1}^{3}m_{ij}\sigma_i^{(1)}\otimes\sigma_j^{(2)}, \tag{60}$$

where $\{\sigma_i\}_{1\leq i\leq 3}$ are the Pauli operators with $\sigma_1\overset{\text{def}}{=}\sigma_x$, $\sigma_2\overset{\text{def}}{=}\sigma_y$, $\sigma_3\overset{\text{def}}{=}\sigma_z$. The terms $\text{H}^{(1)}\otimes\text{I}^{(2)}$ and $\text{I}^{(1)}\otimes\text{H}^{(2)}$ in Eq. (59) represent local interaction Hamiltonians since they act non trivially only on one of the two qubits in the two-qubit quantum state. Clearly, $\text{I}^{(1)}$ and $\text{I}^{(2)}$ denote the identity operators on the first and second subsystems, respectively.

In our first example, we consider the curvature and the torsion of a quantum curve traced out by the initial separable state $\left|00\right\rangle$ under an Hamiltonian H expressed in terms of a superposition of nonlocal two-qubit Hamiltonians,

$$\text{H}\overset{\text{def}}{=}m_1\left(\sigma_x^{(1)}\otimes\sigma_x^{(2)}\right)+m_2\left(\sigma_z^{(1)}\otimes\sigma_z^{(2)}\right)+m_3\left(\sigma_x^{(1)}\otimes\sigma_z^{(2)}\right)+m_4\left(\sigma_z^{(1)}\otimes\sigma_x^{(2)}\right). \tag{61}$$

A straightforward calculation yields distinct curvature and torsion coefficients $\kappa_{\text{AC}}^2=\kappa_{\text{AC}}^2\left(m_1,m_2,m_3,m_4\right)$ and $\tau_{\text{AC}}^2=\tau_{\text{AC}}^2\left(m_1,m_2,m_3,m_4\right)$, respectively, given by

$$\kappa_{\text{AC}}^2=4\frac{\left(m_2^2m_3^2+m_2^2m_4^2+m_3^2m_4^2\right)}{\left(m_1^2+m_3^2+m_4^2\right)^2},\text{ and }\tau_{\text{AC}}^2=4\frac{\left(m_3^2+m_4^2\right)\left(m_1m_2-m_3m_4\right)^2}{\left(m_1^2+m_3^2+m_4^2\right)^3}, \tag{62}$$

with $0\leq\tau_{\text{AC}}^2\leq\kappa_{\text{AC}}^2$ for any choice of the real coupling parameters m_1, m_2, m_3, and m_4. Interestingly, we remark that the quantum curve traced out by the maximally entangled Bell state $\left|\Phi_{\text{Bell}}^+\right\rangle\overset{\text{def}}{=}\left(\left|00\right\rangle+\left|11\right\rangle\right)/\sqrt{2}$ under the Hamiltonian in Eq. (61) is characterized by a nonvanishing curvature coefficient $\kappa_{\text{AC}}^2=4\left[\left(m_1+m_2\right)/\left(m_3-m_4\right)\right]^2$ and a vanishing torsion coefficient $\tau_{\text{AC}}^2=0$. Indeed, it can be checked that under the Hamiltonian in Eq. (61), no curve traced out by any of the remaining three maximally entangled Bell states $\left|\Phi_{\text{Bell}}^-\right\rangle\overset{\text{def}}{=}\left(\left|00\right\rangle-\left|11\right\rangle\right)/\sqrt{2}$, $\left|\Psi_{\text{Bell}}^+\right\rangle\overset{\text{def}}{=}\left(\left|01\right\rangle+\left|10\right\rangle\right)/\sqrt{2}$, and $\left|\Psi_{\text{Bell}}^-\right\rangle\overset{\text{def}}{=}\left(\left|01\right\rangle-\left|10\right\rangle\right)/\sqrt{2}$ exhibits nonzero torsion. For this reason, one may

wonder which might be a suitable two-qubit Hamiltonian to observe some twisting of a quantum curve traced out by evolving a maximally entangled Bell state. We address this question in the next illustrative example.

In our second example, we consider a quantum evolution governed by a two-qubit Hamiltonian H expressed as a superposition of local two-qubit Hamiltonians,

$$\mathrm{H} \overset{\text{def}}{=} m_1 \left(\mathrm{I}^{(1)} \otimes \sigma_x^{(2)} \right) + m_2 \left(\sigma_x^{(1)} \otimes \mathrm{I}^{(2)} \right) + m_3 \left(\mathrm{I}^{(1)} \otimes \sigma_z^{(2)} \right) + m_4 \left(\sigma_z^{(1)} \otimes \mathrm{I}^{(2)} \right). \tag{63}$$

We consider the curvature and the torsion of a quantum curve traced out by the maximally entangled Bell state $\left| \Phi_{\text{Bell}}^+ \right\rangle \overset{\text{def}}{=} \left(\left| 00 \right\rangle + \left| 11 \right\rangle \right) / \sqrt{2}$. A simple calculation leads to identical curvature and torsion coefficients $\kappa_{\text{AC}}^2 = \kappa_{\text{AC}}^2 \left(m_1, m_2, m_3, m_4 \right)$ and $\tau_{\text{AC}}^2 = \tau_{\text{AC}}^2 \left(m_1, m_2, m_3, m_4 \right)$, respectively, given by

$$\kappa_{\text{AC}}^2 = 4 \frac{\left(m_1 m_4 - m_2 m_3 \right)^2}{\left[\left(m_1 + m_2 \right)^2 + \left(m_3 + m_4 \right)^2 \right]^2}, \text{ and } \tau_{\text{AC}}^2 = 4 \frac{\left(m_1 m_4 - m_2 m_3 \right)^2}{\left[\left(m_1 + m_2 \right)^2 + \left(m_3 + m_4 \right)^2 \right]^2}. \tag{64}$$

The presence of identical expressions for κ_{AC}^2 and τ_{AC}^2 in Eq. (64) is a consequence of the fact that the skewness coefficient vanishes in this case (i.e., $\alpha_3 = 0 \leftrightarrow \left\langle \left(\Delta \mathrm{h} \right)^3 \right\rangle = 0$). For completeness, we remark that the curvature $\kappa_{\text{AC}}^2 = \kappa_{\text{AC}}^2 \left(m_1, m_2, m_3, m_4 \right)$ and the torsion $\tau_{\text{AC}}^2 = \tau_{\text{AC}}^2 \left(m_1, m_2, m_3, m_4 \right)$ coefficients of the quantum curve obtained by traced out by the separable state $\left| 00 \right\rangle$ under the Hamiltonian in Eq. (63) are distinct. They are given by

$$\kappa_{\text{AC}}^2 = 4 \frac{\left(m_1^2 m_2^2 + m_1^2 m_3^2 + m_2^2 m_4^2 \right)}{\left(m_1^2 + m_2^2 \right)^2}, \text{ and } \tau_{\text{AC}}^2 = 4 \frac{m_1^2 m_2^2 \left[m_1^2 + m_2^2 + \left(m_3 - m_4 \right)^2 \right]}{\left(m_1^2 + m_2^2 \right)^3}, \tag{65}$$

respectively, with $\kappa_{\text{AC}}^2 - \tau_{\text{AC}}^2 = 4 \left(m_3 m_1^2 + m_4 m_2^2 \right)^2 / \left(m_1^2 + m_2^2 \right)^3$ and $0 \leq \tau_{\text{AC}}^2 \leq \kappa_{\text{AC}}^2$. As evident from Eqs. (64) and (65), the way the curvature and torsion coefficients vary with respect to the tunable (Hamiltonian) parameters depends on both the chosen source state and the selected driving Hamiltonian. This observation paves the way to several intriguing exploratory questions. For instance, in addition to being interested in (shortest length) geodesic quantum evolutions as pointed out in the previous subsubsection, one may be interested in driving a source state along a pre-selected (nongeodesic) path [49, 50]. In this case, the coefficients κ_{AC}^2 and τ_{AC}^2 can be of help in providing useful insights into the behavior of the quantum evolution from a geometric perspective and, in principle, can assist in singling out the proper driving Hamiltonian for the chosen source state that is optimal for the task at hand. Roughly speaking, by tuning the Hamiltonian parameters, one can bend and twist the trajectory traced out by the source state so to avoid obstacles along the path and reach the target state in an optimal manner. Moreover, one could use κ_{AC}^2 and τ_{AC}^2 to geometrically characterize the effects of different degrees of entanglement of quantum states under different quantum Hamiltonian evolutions. In particular, one could find out how difficult and/or easy is to bend and/or twist quantum curves traced out by quantum states with different degrees of entanglement. In Appendix C, we present an example that considers the curvature and torsion coefficients for a quantum curve traced by evolving a three-qubit quantum state, including the $\left| \text{GHZ} \right\rangle$-state and the $\left| \text{W} \right\rangle$-state, under a three-qubit stationary Hamiltonian belonging to the family of the quantum Heisenberg models. For the time being, keeping in mind Feynman's attitude on the use of geometric methods in the study of quantum evolutions [51], we leave a quantitative discussion of these intriguing exploratory lines of investigations to future scientific efforts.

VII.   FINAL REMARKS

In this paper, we proposed a quantum version of the Frenet-Serret apparatus for a quantum trajectory on the generalized Bloch sphere traced out by a parallel-transported pure quantum state $\left| \Psi \left(s \right) \right\rangle$ of arbitrary dimension parametrized in terms of the arc length s that evolves unitarily under a time-independent Hamiltonian specifying the Schrödinger equation (Eq. (16)). Given this parallel-transported unit state vector, we introduced in a proper sequential fashion a suitable pair of two projector operators (i.e., $\mathrm{P}^{(\Psi)}$ and $\mathrm{P}^{(T)} \mathrm{P}^{(\Psi)}$) to construct an intrinsically geometric set of three orthonormal vectors specifying a moving frame associated with the quantum curve $\gamma \left(s \right) : s \mapsto \left| \Psi \left(s \right) \right\rangle$ with $s_i \leq s \leq s_f$. First, we introduce the unit tangent vector as the covariant derivative of the parallel-transported unit state vector (Eq. (20)), $\left| T(s) \right\rangle \overset{\text{def}}{=} \mathrm{P}^{(\Psi)} \left| \Psi' \left(s \right) \right\rangle = \mathrm{D} \left| \Psi \left(s \right) \right\rangle$. The covariant derivative operator $\mathrm{D} \overset{\text{def}}{=} \mathrm{P}^{(\Psi)} (d/ds)$ is defined as the composition of $\mathrm{P}^{(\Psi)}$ and d/ds. The quantity $\mathrm{P}^{(\Psi)}$ is a projection operator onto a state orthogonal to the parallel-transported state vector $\left| \Psi \left(s \right) \right\rangle$, while d/ds denotes the ordinary differential operator with respect to the arc length s. Then, the parallel-transported unit state vector $\left| \Psi \left(s \right) \right\rangle$ and the unit tangent

vector $|T(s)\rangle$ span a two-dimensional space that can be regarded as the quantum analogue of the instantaneous osculating plane in the Frenet-Serret apparatus. Finally, the curvature $\kappa_{\mathrm{AC}}^2(s)$ (Eqs. (21) and (22)) of a quantum curve is defined as the squared magnitude $\|\mathrm{D}\,|T(s)\rangle\|^2$ of the covariant derivative of the unit tangent vector $|T(s)\rangle$ and measures the bending of a quantum curve. Second, to introduce the concept of torsion, we construct a non-normalized vector $\left|\tilde{N}(s)\right\rangle$ (Eq. (25)) that is orthogonal to the instantaneous quantum version of the osculating plane. This third vector is defined as $\mathrm{P}^{(T)}\mathrm{P}^{(\Psi)}|T'(s)\rangle = \mathrm{P}^{(T)}\mathrm{D}\,|T(s)\rangle$, the projection of the derivative with respect to the arc length of the unit tangent vector onto a state that is orthogonal to the plane spanned by the parallel-transported unit state $|\Psi(s)\rangle$ and the unit tangent vector $|T(s)\rangle$. Finally, the torsion τ_{AC}^2 (Eqs. (26) and (27)) of a quantum curve is defined as the squared magnitude $\left\|\mathrm{P}^{(T)}\mathrm{D}\,|T(s)\rangle\right\|^2$ of the projection onto a state orthogonal to the unit tangent vector of the covariant derivative of the unit tangent vector and measures the twisting of a quantum curve. In conclusion, the parallel-transported unit state vector $|\Psi(s)\rangle$, the unit tangent vector $|T(s)\rangle$, and the normalized version of the projection onto a state orthogonal to the unit tangent vector of the covariant derivative of the unit tangent vector, $|N(s)\rangle \overset{\mathrm{def}}{=} \left|\tilde{N}(s)\right\rangle / \left\|\left|\tilde{N}(s)\right\rangle\right\|$, form a quantum version of the Frenet-Serret frame $\left\{\hat{T}, \hat{N}, \hat{B}\right\}$. When adding our proposed concepts of curvature κ_{AC}^2 and torsion τ_{AC}^2 to the three orthonormal vectors $\{|\Psi(s)\rangle, |T(s)\rangle, |N(s)\rangle\}$, we have the set $\left\{|\Psi(s)\rangle, |T(s)\rangle, |N(s)\rangle, \kappa_{\mathrm{AC}}^2(s), \tau_{\mathrm{AC}}^2(s)\right\}$, a quantum version of the Frenet-Serret apparatus $\left\{\hat{T}, \hat{N}, \hat{B}, \kappa_{\mathrm{FS}}(s), \tau_{\mathrm{FS}}(s)\right\}$. Recall that $\kappa_{\mathrm{FS}}^2(s) = \left\|\hat{T}'(s)\right\|^2$, $\tau_{\mathrm{FS}}^2(s) = \left\|\hat{B}'(s)\right\|^2$ are formally defined in Eqs. (12) and (13), respectively. We emphasize that unlike the Frenet-Serret apparatus, we do not have in our theoretical proposal an exact quantum version of the Frenet-Serret equations (Eq. (10)) specified by a closed set of dynamical equations for the FS frame $\left\{\hat{T}, \hat{N}, \hat{B}\right\}$. However, we do have a clear correspondence between our pair $\left(\kappa_{\mathrm{AC}}^2 \overset{\mathrm{def}}{=} \|\mathrm{D}\,|T(s)\rangle\|^2 = \left\|\mathrm{D}^2\,|\Psi(s)\rangle\right\|^2, \tau_{\mathrm{AC}}^2 \overset{\mathrm{def}}{=} \left\|\mathrm{P}^{(T)}\mathrm{D}\,|T(s)\rangle\right\|^2 = \left\|\mathrm{P}^{(T)}\mathrm{D}^2\,|\Psi(s)\rangle\right\|^2\right)$ and the Frenet-Serret pair $\left(\kappa_{\mathrm{FS}}^2 = \left\|\hat{T}'(s)\right\|^2, \tau_{\mathrm{FS}}^2 = \left\|\hat{B}'(s)\right\|^2\right)$. Remarkably, when focusing on time-independent Hamiltonian quantum evolutions, our curvature coefficient κ_{AC}^2 and our torsion coefficient τ_{AC}^2 correspond to the dimensionless curvature and torsion coefficients $\bar{\kappa}_{\mathrm{LT}} \overset{\mathrm{def}}{=} \kappa_{\mathrm{LT}} / \left\langle(\Delta H)^2\right\rangle^2$ (with κ_{LT} in Eq. (4)) and $\bar{\tau}_{\mathrm{LT}} \overset{\mathrm{def}}{=} \tau_{\mathrm{LT}} / \left\langle(\Delta H)^2\right\rangle^2$ (with τ_{LT} in Eq. (8)), respectively, proposed by Laba and Tkachuk in Ref. [7].

Keeping in mind the limitations of our proposed approach as discussed in part of Section V, what is the relevance of our investigation?

[i] It provides a useful set of tools (i.e., quantum frames (Appendix A) along with curvature and torsion coefficients) to characterize quantum evolutions in terms of geometrically intuitive concepts such as bending (related to curvature, Eqs. (21) and (22)) and twisting (related to torsion, Eqs. (26) and (27)).

[ii] It leads (Eqs. (35) and (36)) to relevant physical insights into the underlying statistical structure of quantum theory via concepts like kurtosis, skewness, and Pearson inequality. In particular, geodesic quantum motion specified by a stationary Hamiltonian on the Bloch sphere occurs, from a statistical standpoint, with minimal sharpness (i.e., minimal kurtosis) together with maximal symmetry (i.e., zero skewness). For illustrative details, we refer to Fig. 4.

[iii] It provides an alternative way of quantifying geodesic motion in projective Hilbert space in the framework of geometric quantum mechanics. For instance, curvature (Eq. (22)) as well as geodesic efficiency (Eq. (56)) can be equally used to detect geodesic motion (Eqs. (55) and (58)). For a discussion on the link between the concept of geodesic curvature in classical differential geometry and our proposed curvature coefficient for quantum evolutions, we refer to Appendix B.

[iv] It can provide a way to help to control and manipulate higher-dimensional quantum spin systems by analyzing how the bending and the twisting caused via the application of a given driving Hamiltonian specified by experimentally tunable driving parameters. This can be accomplished by examining the changes in the curvature and torsion depending on the specific degree of entanglement of the quantum state that traces out the curve in projective Hilbert space (Eqs. (62), (64), and (65)).

[v] It can represent a useful platform to study the effects of entanglement on the behavior of curvature and torsion coefficients of curves traced out by quantum states with different degrees of entanglement. For example, from our exploratory investigations (for instance, Eqs. (62), (64), (65), and Appendix C), it seems to be generally false that it is harder to bend and/or twist curves traced out by highly entangled quantum states as one may

be inclined to believe. Indeed, it seems to be the case that the degree of bending and twisting of a quantum curve depends on the specific matching of the pair (source state being driven, driving Hamiltonian).

[vi] Unlike the existing approaches [7, 8], our theoretical construct allows to extend the notions of curvature and torsion coefficients to nonstationary quantum Hamiltonian evolutions in a relatively straightforward manner [32].

In conclusion, regardless of its current limitations, we hope our work will stimulate other researchers and open the way toward further explicit investigations on the interplay between geometry and quantum mechanics. For the time being, we leave a more in-depth quantitative discussion on these potential geometric extensions of our analytical findings, including generalizations to mixed state geometry and time-dependent quantum evolutions of higher-dimensional physical systems, to future scientific endeavors.

Acknowledgments

[1] M. Pettini, *Geometry and Topology in Hamiltonian Dynamics and Statistical Mechanics*, Springer-Verlag New York (2007).

[2] R. Millman and G. Parker, *Elements of Differential Geometry*, Prentice Hall, NY (1977).

[3] O. Consa, *Helical solenoid model of electron*, Progress in Physics **14**, 80 (2018).

[4] M. A. Nielsen and I. L. Chuang, *Quantum Computation and Quantum Information*, Cambridge University Press (2000).

[5] D. B. Brody and L. P. Hughston, *Geometry of quantum statistical inference*, Phys. Rev. Lett. **77**, 2851 (1996).

[6] D. C. Brody and Eva-Marie Graefe, *Information geometry of complex Hamiltonians and exceptional points*, Entropy **15**, 3361 (2013).

[7] H. P. Laba and V. M. Tkachuk, *Geometric characteristics of quantum evolution: Curvature and torsion*, Condensed Matter Physics **20**, 13003 (2017).

[8] Kh. P. Gnatenko, H. P. Laba, and V. M. Tkachuk, *Geometric properties of evolutionary graph states and their detection on a quantum computer*, Phys. Lett. **A452**, 128434 (2022).

[9] I. Zutic, J. Fabian, and S. Das Sarma, *Spintronics: Fundamentals and applications*, Rev. Mod. Phys. 76, 323 (2004).

[10] R. Hanson, L. P. Kouwenhoven, J. R. Petta, S. Tarucha, and L. M. K. Vandersypen, *Spins in few-electron quantum dots*, Rev. Mod. Phys. **79**, 1217 (2007).

[11] C. Cafaro and P. M. Alsing, *Complexity of pure and mixed qubit geodesic paths on curved manifolds*, Phys. Rev. **D106**, 096004 (2022)

[12] C. Cafaro, S. Ray, and P. M. Alsing, *Complexity and efficiency of minimum entropy production probability paths from quantum dynamical evolutions*, Phys. Rev. **E105**, 034143 (2022).

[13] C. Cafaro and P. M. Alsing, *Continuous-time quantum search and time-dependent two-level quantum systems*, Int. J. Quantum Information **17**, 1950025 (2019).

[14] C. Cafaro, S. Ray, and P. M. Alsing, *Geometric aspects of analog quantum search evolutions*, Phys. Rev. **A102**, 052607 (2020).

[15] C. Cafaro and P. M. Alsing, *Qubit geodesics on the Bloch sphere from optimal-speed Hamiltonian evolutions*, Class. Quantum Grav. **40**, 115005 (2023).

[16] I. Bengtsson and K. Zyczkowski, *Geometry of Quantum States*, Cambridge University Press (2017).

[17] E. Kreyszig, *Differential Geometry*, Dover Publications (1991).

[18] D. Kazaras and I. Sterling, *An explicit formula for spherical curves with constant torsion*, Pacific Journal of Mathematics **259**, 361 (2012).

[19] P. Erdös, *Spiraling the Earth with C. G. J. Jacobi*, Am. J. Phys. **68**, 888 (2000).

[20] J. Samuel and R. Bhandari, *General setting for Berry's phase*, Phys. Rev. Lett. **60**, 2339 (1988).

[21] P. M. Alsing, C. Cafaro, O. Luongo, C. Lupo, S. Mancini, and H. Quevedo, *Comparing metrics for mixed quantum states: Sjöqvist and Bures*, Phys. Rev. **A107**, 052411 (2023).

[22] J. Ernest Wilkins, Jr., *A note on skewness and kurtosis*, Ann. Math. Stat. **15**, 333 (1944).

[23] R. Sharma and R. Bhandari, *Skewness, kurtosis and Newton's inequality*, Rocky Mountain Journal of Mathematics **45**, 1639 (2015).

[24] K. Pearson, *Mathematical contributions to the theory of evolution, XIX; Second supplement to a memoir on skew variation*, Phil. Trans. Roy. Soc. Lond. **A216**, 432 (1916).

[25] L. Jakobczyk and M. Siennicki, *Geometry of Bloch vectors in two-qubit system*, Phys. Lett. **A286**, 383 (2001).

[26] G. Kimura, *The Bloch vector for N-level systems*, Phys. Lett. **A314**, 339 (2003).

[27] R. A. Bertlmann and P. Krammer, *Bloch vectors for qudits*, J. Phys. A: Math. Theor. **41**, 235303 (2008).

[28] P. Kurzynski, *Multi-Bloch vector representation of the qutrit*, Quantum Inf. Comp. **11**, 361 (2011).

[29] J. Xie et *al.*, *Observing geometry of quantum states in a three-level system*, Phys. Rev. Lett. **125**, 150401 (2020).

[30] C. Eltschka, M. Huber, S. Morelli, and J. Siewert, *The shape of higher-dimensional state space: Bloch-ball analog for a qutrit*, Quantum **5**, 485 (2021).

[31] O. Gamel, *Entangled Bloch spheres: Bloch matrix and two-qubit state space*, Phys. Rev. **A93**, 062320 (2016).

[32] P. M. Alsing and C. Cafaro, *From the classical Frenet-Serret apparatus to the curvature and torsion of quantum-mechanical evolutions. Part II. Nonstationary Hamiltonians*, arXiv:quant-ph/2311.18463 (2023).

[33] L. Landau, *A theory of energy transfer. II*, Phys. Z. Sowjet **2**, 46 (1932).

[34] C. Zener, *Non-adiabatic crossing of energy levels*, Proc. R. Soc. **A137**, 696 (1932).

[35] I. I. Rabi, *Space quantization in a gyrating magnetic field*, Phys. Rev. **51**, 652 (1937).

[36] I. I. Rabi, N. F. Ramsey, and J. Schwinger, *Use of rotating coordinates in magnetic resonance problems*, Rev. Mod. Phys. **26**, 167 (1954).

[37] E. Barnes and S. Das Sarma, *Analytically solvable driven time-dependent two-level quantum systems*, Phys. Rev. Lett. **109**, 060401 (2012).

[38] E. Barnes, *Analytically solvable two-level quantum systems and Landau-Zener interferometry*, Phys. Rev. **A88**, 013818 (2013).

[39] A. Messina and H. Nakazato, *Analytically solvable Hamiltonians for quantum two-level systems and their dynamics*, J. Phys. A: Math and Theor. **47**, 44302 (2014).

[40] R. Grimaudo, A. S. Magalhaes de Castro, H. Nakazato, and A. Messina, *Classes of exactly solvable generalized semi-classical Rabi systems*, Annalen der Physik **530**, 1800198 (2018).

[41] A. S. Magalhaes de Castro, R. Grimaudo, D. Valenti, A. Migliore, H. Nakazato, and A. Messina, *Analytically solvable Hamiltonian in invariant subspaces*, Eur. Phys. J. Plus **138**, 766 (2023).

[42] E. R. Loubenets and C. Kading, *Specifying the unitary evolution of a qudit for a general nonstationary Hamiltonian via the generalized Gell-Mann representation*, Entropy **22**, 521 (2020).

[43] B. O'Neill, *Elementary Differential Geometry*, Elsevier Academic Press (2006).

[44] J. Alvarez-Vizoso, R. Arn, M. Kirby, C. Peterson, and B. Draper, *Geometry of curves in $\mathbb{R}^n$ from the local singular value decomposition*, Lin. Algebra Appl. **571**, 180 (2019).

[45] R. L. Bishop, *There is more than one way to frame a curve*, Amer. Math. Montly **82**, 246 (1975).

[46] A. Mostafazadeh, *Hamiltonians generating optimal-speed evolutions*, Phys. Rev. **A79**, 014101 (2009).

[47] J. Anandan and Y. Aharonov, *Geometry of quantum evolution*, Phys. Rev. Lett. **65**, 1697 (1990).

[48] C. H. Bennett, J. I. Cirac, M. S. Leifer, D. W. Leung, N. Linden, S. Popescu, and G. Vidal, *Optimal simulation of two-qubit Hamiltonians using general local operations*, Phys. Rev. **A66**, 012305 (2002).

[49] R. Uzdin, U. Gunther, S. Rahav, and N. Moiseyev, *Time-dependent Hamiltonians with 100% evolution speed efficiency*, J. Phys. **A**: Math. Theor. **45**, 415304 (2012).

[50] F. Campaioli, W. Sloan, K. Modi, and F. A. Pollock, *Algorithm for solving unconstrained unitary quantum brachistochrone problems*, Phys. Rev. **A100**, 062328 (2019).

[51] R. P. Feynman, F. L. Vernon, and R. W. Hellwarth, *Geometrical representation of the Schrödinger equation for solving maser problems*, J. Appl. Phys. **28**, 49 (1957).

[52] D. P. Landau and K. Binder, *A Guide to Monte Carlo Simulations in Statistical Physics*, Cambridge University Press (2005).

Appendix A: Framing a quantum curve

In this Appendix, following our suggestion in Section V, we present an illustrative example on how to frame a quantum curve. Specifically, we wish to construct the frame for the quantum curve traced by evolving the two-qubit quantum state $|\psi(0)\rangle = |00\rangle$ under the stationary Hamiltonian $\mathrm{H} \overset{\mathrm{def}}{=} \sigma_x^{(1)} \otimes \sigma_x^{(2)} + \sigma_z^{(1)} \otimes \sigma_x^{(2)}$. Using the statistical approach based upon the calculation of expectation values in Eqs. (24) and (29), it is straightforward to verify that $\kappa_{\mathrm{AC}}^2 = \tau_{\mathrm{AC}}^2 = 1$ in this case. Since the Hilbert space $\mathcal{H}_2^2$ of two-qubit quantum states is four-dimensional, we want to get a frame specified by a set of orthonormal vectors given by $\{|\Psi(s)\rangle, |T(s)\rangle, |N(s)\rangle, |V(s)\rangle\}$. We begin by observing that the unitary time evolution operator $\mathcal{U}(t) \overset{\mathrm{def}}{=} e^{-i\mathrm{H}t}$ that corresponds to $\mathrm{H} \overset{\mathrm{def}}{=} \sigma_x^{(1)} \otimes \sigma_z^{(2)} + \sigma_z^{(1)} \otimes \sigma_x^{(2)}$ is given by,

$$
\mathcal{U}(t) = \begin{pmatrix}
\frac{1}{4e^{2it}}\left(e^{2it}+1\right)^2 & -\frac{1}{4e^{2it}}\left(e^{4it}-1\right) & -\frac{1}{4e^{2it}}\left(e^{4it}-1\right) & -\frac{1}{4e^{2it}}\left(e^{2it}-1\right)^2 \\
-\frac{1}{4e^{2it}}\left(e^{4it}-1\right) & \frac{1}{4e^{2it}}\left(e^{2it}+1\right)^2 & \frac{1}{4e^{2it}}\left(e^{2it}-1\right)^2 & \frac{1}{4e^{2it}}\left(e^{4it}-1\right) \\
-\frac{1}{4e^{2it}}\left(e^{4it}-1\right) & \frac{1}{4e^{2it}}\left(e^{2it}-1\right)^2 & \frac{1}{4e^{2it}}\left(e^{2it}+1\right)^2 & \frac{1}{4e^{2it}}\left(e^{4it}-1\right) \\
-\frac{1}{4e^{2it}}\left(e^{2it}-1\right)^2 & \frac{1}{4e^{2it}}\left(e^{4it}-1\right) & \frac{1}{4e^{2it}}\left(e^{4it}-1\right) & \frac{1}{4e^{2it}}\left(e^{2it}+1\right)^2
\end{pmatrix},
\tag{A1}
$$

where we have set $\hbar$ equal to one. From Eq. (A1), the evolved state $|\psi(t)\rangle = \mathcal{U}(t)|\psi(0)\rangle$ becomes

$$
|\psi(t)\rangle = \cos^2(t)|00\rangle - \frac{i}{2}\sin(2t)|01\rangle - \frac{i}{2}\sin(2t)|10\rangle + \sin^2(t)|11\rangle.
\tag{A2}
$$

We note that since $\langle \mathrm{H} \rangle = 0$, we have $|\Psi(t)\rangle = |\psi(t)\rangle$. Moreover, since $\langle(\Delta\mathrm{H})^2\rangle = 2$, we have $s = \sqrt{2}t$. Therefore, $t = s/\sqrt{2}$ and $|\Psi(s)\rangle$ becomes

$$
|\Psi(s)\rangle = \cos^2\left(\frac{s}{\sqrt{2}}\right)|00\rangle - \frac{i}{2}\sin\left(\sqrt{2}s\right)|01\rangle - \frac{i}{2}\sin\left(\sqrt{2}s\right)|10\rangle + \sin^2\left(\frac{s}{\sqrt{2}}\right)|11\rangle.
\tag{A3}
$$

Using Eq. (A3), the expressions for $|T(s)\rangle$ and $|T'(s)\rangle$ are given by

$$
|T(s)\rangle = -\frac{1}{\sqrt{2}}\sin\left(\sqrt{2}s\right)|00\rangle - \frac{i}{\sqrt{2}}\cos\left(\sqrt{2}s\right)|01\rangle - \frac{i}{\sqrt{2}}\cos\left(\sqrt{2}s\right)|10\rangle + \frac{1}{\sqrt{2}}\sin\left(\sqrt{2}s\right)|11\rangle,
\tag{A4}
$$

and

$$
|T'(s)\rangle = -\cos(\sqrt{2}s)|00\rangle + i\sin(\sqrt{2}s)|01\rangle + i\sin(\sqrt{2}s)|10\rangle + \cos\left(\sqrt{2}s\right)|11\rangle,
\tag{A5}
$$

respectively. For completeness, we remark that $|\Psi(t)\rangle$ and $|T(s)\rangle$ are normalized to one and they are orthogonal. We need to find now $|N(s)\rangle \overset{\mathrm{def}}{=} \mathrm{P}^{(T)}\mathrm{P}^{(\Psi)}|T'(s)\rangle / \|\mathrm{P}^{(T)}\mathrm{P}^{(\Psi)}|T'(s)\rangle\|$. Therefore, we need to calculate the projectors $\mathrm{P}^{(\Psi)} \overset{\mathrm{def}}{=} \mathrm{I}_{\mathcal{H}_2^2} - |\Psi\rangle\langle\Psi|$ and $\mathrm{P}^{(T)} \overset{\mathrm{def}}{=} \mathrm{I}_{\mathcal{H}_2^2} - |T\rangle\langle T|$. Using Eqs. (A3) and (A4), we get that $\mathrm{P}^{(\Psi)}$ and $\mathrm{P}^{(T)}$ are given by

$$
\mathrm{P}^{(\Psi)} = \begin{pmatrix}
1 - \cos^4\left(\frac{s}{\sqrt{2}}\right) & -\frac{i}{2}\sin\left(\sqrt{2}s\right)\cos^2\left(\frac{s}{\sqrt{2}}\right) & -\frac{i}{2}\sin\left(\sqrt{2}s\right)\cos^2\left(\frac{s}{\sqrt{2}}\right) & -\sin^2\left(\frac{s}{\sqrt{2}}\right)\cos^2\left(\frac{s}{\sqrt{2}}\right) \\
\frac{i}{2}\sin\left(\sqrt{2}s\right)\cos^2\left(\frac{s}{\sqrt{2}}\right) & 1 - \frac{1}{4}\sin^2\left(\sqrt{2}s\right) & -\frac{1}{4}\sin^2\left(\sqrt{2}s\right) & \frac{i}{2}\sin\left(\sqrt{2}s\right)\sin^2\left(\frac{s}{\sqrt{2}}\right) \\
\frac{i}{2}\sin\left(\sqrt{2}s\right)\cos^2\left(\frac{s}{\sqrt{2}}\right) & -\frac{1}{4}\sin^2\left(\sqrt{2}s\right) & 1 - \frac{1}{4}\sin^2\left(\sqrt{2}s\right) & \frac{i}{2}\sin\left(\sqrt{2}s\right)\sin^2\left(\frac{s}{\sqrt{2}}\right) \\
-\sin^2\left(\frac{s}{\sqrt{2}}\right)\cos^2\left(\frac{s}{\sqrt{2}}\right) & -\frac{i}{2}\sin\left(\sqrt{2}s\right)\sin^2\left(\left(\frac{s}{\sqrt{2}}\right)\right) & -\frac{i}{2}\sin\left(\sqrt{2}s\right)\sin^2\left(\left(\frac{s}{\sqrt{2}}\right)\right) & 1 - \sin^4\left(\frac{s}{\sqrt{2}}\right)
\end{pmatrix},
\tag{A6}
$$

and

$$
\mathrm{P}^{(T)} = \begin{pmatrix}
1 - \frac{1}{2}\sin^2\left(\sqrt{2}s\right) & \frac{i}{2}\sin\left(\sqrt{2}s\right)\cos\left(\sqrt{2}s\right) & \frac{i}{2}\sin\left(\sqrt{2}s\right)\cos\left(\sqrt{2}s\right) & \frac{1}{2}\sin^2\left(\sqrt{2}s\right) \\
-\frac{i}{2}\sin\left(\sqrt{2}s\right)\cos\left(\sqrt{2}s\right) & 1 - \frac{1}{2}\cos^2\left(\sqrt{2}s\right) & -\frac{1}{2}\cos^2\left(\sqrt{2}s\right) & \frac{i}{2}\sin\left(\sqrt{2}s\right)\cos\left(\sqrt{2}s\right) \\
-\frac{i}{2}\sin\left(\sqrt{2}s\right)\cos\left(\sqrt{2}s\right) & -\frac{1}{2}\cos^2\left(\sqrt{2}s\right) & 1 - \frac{1}{2}\cos^2\left(\sqrt{2}s\right) & \frac{i}{2}\sin\left(\sqrt{2}s\right)\cos\left(\sqrt{2}s\right) \\
\frac{1}{2}\sin^2\left(\sqrt{2}s\right) & -\frac{i}{2}\sin\left(\sqrt{2}s\right)\cos\left(\sqrt{2}s\right) & -\frac{i}{2}\sin\left(\sqrt{2}s\right)\cos\left(\sqrt{2}s\right) & 1 - \frac{1}{2}\sin^2\left(\sqrt{2}s\right)
\end{pmatrix}, \tag{A7}
$$

respectively. As a consistency check, we verified that $\mathrm{P}^{(\Psi)}$ and $\mathrm{P}^{(T)}$ are proper orthogonal projectors. Additionally, to evaluate κ_{AC}^2 by using the definition itself of curvature coefficient (i.e., $\kappa_{\mathrm{AC}}^2 = \|\mathrm{P}^{(\Psi)}|T'(s)\rangle\|^2$), we note that

$$
\mathrm{P}^{(\Psi)}|T'(s)\rangle = \begin{pmatrix}
\frac{1}{2} - \frac{1}{2}\cos\left(\sqrt{2}s\right) \\
\frac{1}{2}i\sin\left(\sqrt{2}s\right) \\
\frac{1}{2}i\sin\left(\sqrt{2}s\right) \\
\frac{1}{2}\cos\left(\sqrt{2}s\right) + \frac{1}{2}
\end{pmatrix},
\tag{A8}
$$

and, thus, $\kappa_{\mathrm{AC}}^2 = 1$. In addition, to evaluate τ_{AC}^2 by using the definition itself of torsion coefficient (i.e., $\tau_{\mathrm{AC}}^2 = \left\| \mathrm{P}^{(T)} \mathrm{P}^{(\Psi)} \left| T'(s) \right\rangle \right\|^2$), we note that

$$\mathrm{P}^{(T)} \mathrm{P}^{(\Psi)} \left| T'(s) \right\rangle = \begin{pmatrix} \frac{1}{2} - \frac{1}{2} \cos\left(\sqrt{2}s\right) \\ \frac{1}{2} i \sin\left(\sqrt{2}s\right) \\ \frac{1}{2} i \sin\left(\sqrt{2}s\right) \\ \frac{1}{2} \cos\left(\sqrt{2}s\right) + \frac{1}{2} \end{pmatrix}, \tag{A9}$$

that is, $\tau_{\mathrm{AC}}^2 = 1$. Finally, the vector $\left| N(s) \right\rangle$ reduces to

$$\left| N(s) \right\rangle \overset{\mathrm{def}}{=} \frac{\mathrm{P}^{(T)} \mathrm{P}^{(\Psi)} \left| T'(s) \right\rangle}{\left\| \mathrm{P}^{(T)} \mathrm{P}^{(\Psi)} \left| T'(s) \right\rangle \right\|} = \begin{pmatrix} \frac{1}{2} - \frac{1}{2} \cos\left(\sqrt{2}s\right) \\ \frac{1}{2} i \sin\left(\sqrt{2}s\right) \\ \frac{1}{2} i \sin\left(\sqrt{2}s\right) \\ \frac{1}{2} \cos\left(\sqrt{2}s\right) + \frac{1}{2} \end{pmatrix}, \tag{A10}$$

that is

$$\left| N(s) \right\rangle = \left[\frac{1}{2} - \frac{1}{2} \cos\left(\sqrt{2}s\right) \right] \left| 00 \right\rangle + \frac{i}{2} \sin\left(\sqrt{2}s\right) \left| 01 \right\rangle + \frac{i}{2} \sin\left(\sqrt{2}s\right) \left| 10 \right\rangle + \left[\frac{1}{2} \cos\left(\sqrt{2}s\right) + \frac{1}{2} \right] \left| 11 \right\rangle. \tag{A11}$$

We point out that we checked that $\left| N(s) \right\rangle$ is normalized to one and orthogonal to both $\left| \Psi(s) \right\rangle$ and $\left| T(s) \right\rangle$. To find an orthonormal basis of $\mathcal{H}_2^2$, we note that (by educated guess) $\{ \left| \Psi(s) \right\rangle, \left| T(s) \right\rangle, \left| N(s) \right\rangle, \left| 01 \right\rangle \}$ is a set of linearly independent vectors. Then, applying the Gram-Schmidt procedure, we find that an orthonormal basis of $\mathcal{H}_2^2$ is given by $\{ \left| \Psi(s) \right\rangle, \left| T(s) \right\rangle, \left| N(s) \right\rangle, \left| V(s) \right\rangle \}$ with $\left| V(s) \right\rangle$ given by

$$\left| V(s) \right\rangle \overset{\mathrm{def}}{=} \frac{\left| 01 \right\rangle - \left\langle \Psi(s) \left| 01 \right\rangle \right. \left| \Psi(s) \right\rangle + \left\langle T(s) \left| 01 \right\rangle \right. \left| T(s) \right\rangle + \left\langle N(s) \left| 01 \right\rangle \right. \left| N(s) \right\rangle}{\left\| \left| 01 \right\rangle - \left\langle \Psi(s) \left| 01 \right\rangle \right. \left| \Psi(s) \right\rangle + \left\langle T(s) \left| 01 \right\rangle \right. \left| T(s) \right\rangle + \left\langle N(s) \left| 01 \right\rangle \right. \left| N(s) \right\rangle \right\|} = \frac{\left| 01 \right\rangle - \left| 10 \right\rangle}{\sqrt{2}}. \tag{A12}$$

For completeness, we point out that we checked explicitly that $\{ \left| \Psi(s) \right\rangle, \left| T(s) \right\rangle, \left| N(s) \right\rangle, \left| V(s) \right\rangle \}$ is a set of four orthonormal vectors. Finally, restricting our attention to the three-dimensional subspace of $\mathcal{H}_2^2$ spanned by the orthonormal quantum frame $\{ \left| \Psi(s) \right\rangle, \left| T(s) \right\rangle, \left| N(s) \right\rangle \}$ with $\left| \Psi(s) \right\rangle$ in Eq. (A3), $\left| T(s) \right\rangle$ in Eq. (A4), and $\left| N(s) \right\rangle$ in Eq. (A11), we have that the coefficient matrix $\mathrm{M}_{\partial_s(\mathrm{Frame}) \to \mathrm{Frame}}^{(\mathrm{FS})}$ that expresses the derivatives of the frame with respect to the curve parameter s in terms of the frame itself is given by

$$\begin{pmatrix} \partial_s \left| \Psi(s) \right\rangle \\ \partial_s \left| T(s) \right\rangle \\ \partial_s \left| N(s) \right\rangle \end{pmatrix} = \begin{pmatrix} 0 & 1 & 0 \\ -1 & 0 & 1 \\ 0 & -1 & 0 \end{pmatrix} \begin{pmatrix} \left| \Psi(s) \right\rangle \\ \left| T(s) \right\rangle \\ \left| N(s) \right\rangle \end{pmatrix}. \tag{A13}$$

Interestingly, we note that $\mathrm{M}_{\partial_s(\mathrm{Frame}) \to \mathrm{Frame}}^{(\mathrm{FS})}$ in Eq. (A13) is real and exhibits the skew-symmetric property, despite the fact that curvature and torsion coefficients are nonzero in this case. Indeed, the generally skew-Hermitian matrix $\mathrm{M}_{\partial_s(\mathrm{Frame}) \to \mathrm{Frame}}^{(\mathrm{FS})}$ in Eq. (50) becomes the skew-symmetric one in Eq. (A13) in this scenario because $\kappa_{\mathrm{AC}}^2 = \tau_{\mathrm{AC}}^2 = 1$, $\phi_{\langle N | T' \rangle} = 0$, and $\mathrm{Im}\left(\left\langle N | N' \right\rangle \right) = 0$. Finally, we point out that $\mathrm{Span}\{ \left| \Psi(s) \right\rangle, \left| T(s) \right\rangle, \left| N(s) \right\rangle \}$ is equal to $\mathrm{Span}\{ \partial_s \left| \Psi(s) \right\rangle, \partial_s \left| T(s) \right\rangle, \partial_s \left| N(s) \right\rangle \}$. This is an important remark since we are formally considering curves on "generalized Bloch spheres" embedded in the four-dimensional complex Hilbert space $\mathcal{H}_2^2$ and the three-dimensional subspace spanned by the frame fields is big enough to accommodate the derivatives of the frame fields as well.

Appendix B: Link between geodesic curvature and κ_{AC}^2

In this Appendix, we point out the connection between the concept of geodesic curvature κ_{geo} in differential geometry and our proposed curvature coefficient κ_{AC}^2. We begin by remarking that care is required when studying curvature aspects of a curve [17]. For example, the curvature of a circle on a plane is an intrinsic property of the circle. Instead, the curvature of a circle on a spherical surface is an extrinsic property of the circle. Consider a circle of radius R. When this circle is considered as a great circle on a sphere, it has geodesic curvature κ_{geo} equal to zero. Clearly, if the circle lies on the sphere but is not a great sphere, its geodesic curvature κ_{geo} differs from zero. For a discussion on spherical curves on a sphere embedded in three-dimensions, we refer to Refs. [18, 19]. Moreover, when the circle

is viewed as a curve in a plane, its curvature κ_{FS} is $1/R$, with κ_{FS} as introduced within the Frenet-Serret apparatus for a curve in three-dimensional physical space [17]. The curvature κ_{FS} and torsion coefficients τ_{FS} for a curve γ in three-dimensional Euclidean space defined by the vector relation $\vec{r} = \vec{r}(s)$ with s being the arc length of γ are given by

$$\kappa_{\mathrm{FS}}(s) \overset{\text{def}}{=} \frac{\|\vec{r}' \times \vec{r}''\|}{\|\vec{r}'\|^3}, \text{ and } \tau_{\mathrm{FS}}(s) \overset{\text{def}}{=} \frac{(\vec{r}' \times \vec{r}'') \cdot \vec{r}'''}{\|\vec{r}' \times \vec{r}''\|^2}, \tag{B1}$$

respectively, with $\vec{r}' \overset{\text{def}}{=} d\vec{r}/ds$. Alternatively, consider a curve $\tilde{\gamma}$ on a surface S embedded in a three-dimensional Euclidean space specified by the vectorial relation $\vec{r} = \vec{r}(u^1(s), u^2(s))$ with s being the arc length of $\tilde{\gamma}$. Let $\hat{n}$ and $\hat{t}$ be the unit normal and unit tangent vectors to S at a point P of $\tilde{\gamma}$, respectively. Let $\hat{b} \overset{\text{def}}{=} \hat{n} \times \hat{t}$ be the unit vector orthogonal to both $\hat{n}$ and $\hat{t}$. Then, the curvature vector $\vec{\kappa}$ of $\tilde{\gamma}$ at P is the vector sum of the normal curvature vector $\kappa_n \hat{n}$ and the geodesic curvature vector $\kappa_{\mathrm{geo}} \hat{b}$ and is defined as,

$$\vec{\kappa} \overset{\text{def}}{=} \kappa_n \hat{n} + \kappa_{\mathrm{geo}} \hat{b}. \tag{B2}$$

The scalar quantities $\kappa_n(s) \overset{\text{def}}{=} \vec{r}'' \cdot \hat{n}$ and $\kappa_{\mathrm{geo}}(s) \overset{\text{def}}{=} \vec{r}'' \cdot \hat{b}$ are the normal and the geodesic curvatures, respectively. As an illustrative example, consider a spherical curve γ on a sphere of radius $R > 0$ and centered at the origin. More specifically, using spherical coordinates (with $\theta_\xi \in [0, \pi]$ being the polar angle as in the main paper), assume to consider a circle at $z = \cos(\theta_\xi)$ and parametrized by the arc length s as

$$\vec{r}(s) = \left(R \sin(\theta_\xi) \cos(\frac{s}{R \sin(\theta_\xi)}), R \sin(\theta_\xi) \sin(\frac{s}{R \sin(\theta_\xi)}), R \cos(\theta_\xi) \right). \tag{B3}$$

Note that $\vec{r}(s)$ in Eq. (B3) yields a unit-speed parametrization since $\|\vec{r}'(s)\|^2 = 1$. Substituting Eq. (B3) into Eq. (B1) leads to $\tau_{\mathrm{FS}}(s) = 0$ and $\kappa_{\mathrm{FS}}(s) = 1/[R \sin(\theta_\xi)]$. Moreover, use of $\vec{r}(s)$ into $\kappa_{\mathrm{geo}}(s) \overset{\text{def}}{=} \vec{r}'' \cdot \hat{b}$ with $\hat{b} = \vec{r}/\|\vec{r}\|$ gives $\kappa_{\mathrm{geo}} = \cot(\theta_\xi)/R$, that is, $\kappa_{\mathrm{geo}}^2 \sim \cos^2(\theta_\xi)/\sin^2(\theta_\xi)$. Thus, $\kappa_{\mathrm{geo}}^2 \sim \kappa_{\mathrm{AC}}^2$ in Eq. (55). With this interesting conclusive remark, we end our discussion here.

Appendix C: Curvature, torsion, and the quantum Heisenberg model

In this Appendix, in addition to the illustrative examples discussed in Section VI, we report an example that considers the curvature and torsion coefficients for a quantum curve traced by evolving a three-qubit quantum state, including the $|GHZ\rangle$-state (Greenberger-Horne-Zeilinger) and the $|W\rangle$-state (Wolfgang Dür), under a three-qubit stationary Hamiltonian belonging to the family of the quantum Heisenberg models.

The quantum Heisenberg model (QHM) is a model of magnetic spin systems used in statistical mechanics to study thermodynamics aspects of the system [52]. In this model, magnetic spins are treated quantum-mechanically and, therefore, they are expressed by quantum operators and not by classical vectors. For a system of N spin-1/2 particles with a nearest-neighbours interaction and immersed in a uniform magnetic field $\vec{B} = h\hat{z}$, the QHM is given by

$$\mathrm{H} \overset{\text{def}}{=} \sum_{j=1}^{N} \left(J_x \sigma_x^{(j)} \sigma_x^{(j+1)} + J_y \sigma_y^{(j)} \sigma_y^{(j+1)} + J_z \sigma_z^{(j)} \sigma_z^{(j+1)} + h \sigma_z^{(j)} \right), \tag{C1}$$

where $\sigma_a^{(j)} = \mathrm{I}^{\otimes j-1} \otimes \sigma_a^{(j)} \otimes \mathrm{I}^{\otimes N-j}$, $a \in \{x, y, z\}$, $1 \leq j \leq N$, I is the 2×2 identity matrix, and $\sigma_{N+1} = \sigma_1$ is the usual periodic boundary condition. The real quantities J_x, J_y, and J_z are the coupling constants. When $J_x \neq J_y \neq J_z$, one has the Heisenberg XYZ model. Furthermore, when $J_x = J_y \neq J_z$, one has the Heisenberg XXZ model. Finally, when $J_x = J_y = J_z$, one has the Heisenberg XXX model. For the XXX model, $J_x > 0$ and $J_x < 0$ correspond to the antiferromagnetic and ferromagnetic scenarios, respectively. In our explicit example, we focus on a special case of Eq. (C1) specified by the Hamiltonian

$$\begin{aligned}
\mathrm{H} \overset{\text{def}}{=} & J_x \left(\sigma_x^{(1)} \otimes \sigma_x^{(2)} \otimes \mathrm{I}^{(3)} + \sigma_x^{(1)} \otimes \mathrm{I}^{(2)} \otimes \sigma_x^{(3)} + \mathrm{I}^{(1)} \otimes \sigma_x^{(2)} \otimes \sigma_x^{(3)} \right) \\
& + J_y \left(\sigma_y^{(1)} \otimes \sigma_y^{(2)} \otimes \mathrm{I}^{(3)} + \sigma_y^{(1)} \otimes \mathrm{I}^{(2)} \otimes \sigma_y^{(3)} + \mathrm{I}^{(1)} \otimes \sigma_y^{(2)} \otimes \sigma_y^{(3)} \right) \\
& + J_z \left(\sigma_z^{(1)} \otimes \sigma_z^{(2)} \otimes \mathrm{I}^{(3)} + \sigma_z^{(1)} \otimes \mathrm{I}^{(2)} \otimes \sigma_z^{(3)} + \mathrm{I}^{(1)} \otimes \sigma_z^{(2)} \otimes \sigma_z^{(3)} \right) \\
& + h \left(\sigma_z^{(1)} \otimes \mathrm{I}^{(2)} \otimes \mathrm{I}^{(3)} + \mathrm{I}^{(1)} \otimes \sigma_z^{(2)} \otimes \mathrm{I}^{(3)} + \mathrm{I}^{(1)} \otimes \mathrm{I}^{(2)} \otimes \sigma_z^{(3)} \right),
\end{aligned} \tag{C2}$$

that is, in the canonical (8×8)-matrix notation,

$$
\text{H} = \begin{pmatrix}
3h + 3J_z & 0 & 0 & J_x - J_y & 0 & J_x - J_y & J_x - J_y & 0 \\
0 & h - J_z & J_x + J_y & 0 & J_x + J_y & 0 & 0 & J_x - J_y \\
0 & J_x + J_y & h - J_z & 0 & J_x + J_y & 0 & 0 & J_x - J_y \\
J_x - J_y & 0 & 0 & -h - J_z & 0 & J_x + J_y & J_x + J_y & 0 \\
0 & J_x + J_y & J_x + J_y & 0 & h - J_z & 0 & 0 & J_x - J_y \\
J_x - J_y & 0 & 0 & J_x + J_y & 0 & -h - J_z & J_x + J_y & 0 \\
J_x - J_y & 0 & 0 & J_x + J_y & 0 & J_x + J_y & -h - J_z & 0 \\
0 & J_x - J_y & J_x - J_y & 0 & J_x - J_y & 0 & 0 & 3J_z - 3h
\end{pmatrix}. \tag{C3}
$$

In our first sub-case, assume that H in Eq. (C3) is the driving Hamiltonian and the source state to be driven is the entangled quantum state of three qubits given by $|GHZ\rangle \overset{\text{def}}{=} [|000\rangle + |111\rangle]/\sqrt{2}$. Then, after some tedious but straightforward calculations, it happens that the curvature κ_{AC}^2 and torsion τ_{AC}^2 coefficients are given by

$$
\kappa_{\text{AC}}^2 (J_x, J_y, J_z, h) = \frac{4}{3} (J_x - J_y)^2 \frac{h^2 + [(J_x + J_y) - 2J_z]^2}{\left[3h^2 + (J_x - J_y)^2\right]^2}, \tag{C4}
$$

and,

$$
\tau_{\text{AC}}^2 (J_x, J_y, J_z, h) = \frac{4}{3} (J_x - J_y)^2 \frac{h^2 + [(J_x + J_y) - 2J_z]^2}{\left[3h^2 + (J_x - J_y)^2\right]^2} - \frac{4}{3} (J_x - J_y)^4 \frac{[(J_x + J_y) - 2J_z]^2}{\left[3h^2 + (J_x - J_y)^2\right]^3}, \tag{C5}
$$

respectively. As a sanity check, note from Eqs. (C4) and (C5) that $0 \leq \tau_{\text{AC}}^2 (J_x, J_y, J_z, h) \leq \kappa_{\text{AC}}^2 (J_x, J_y, J_z, h)$ since we have the following chain of inequalities,

$$
\frac{4}{3} (J_x - J_y)^2 \frac{h^2 + [(J_x + J_y) - 2J_z]^2}{\left[3h^2 + (J_x - J_y)^2\right]^2} \geq \frac{4}{3} (J_x - J_y)^2 \frac{[(J_x + J_y) - 2J_z]^2}{\left[3h^2 + (J_x - J_y)^2\right]^2} \geq \frac{4}{3} (J_x - J_y)^4 \frac{[(J_x + J_y) - 2J_z]^2}{\left[3h^2 + (J_x - J_y)^2\right]^3}. \tag{C6}
$$

The last inequality in Eq. (C6) is true since it is equivalent to

$$
\frac{(J_x - J_y)^2}{3h^2 + (J_x - J_y)^2} \leq 1, \tag{C7}
$$

which is obviously satisfied since $3h^2 \geq 0$. In our second sub-case, assume that H in Eq. (C3) is the driving Hamiltonian and the source state to be driven is the entangled quantum state of three qubits given by $|W\rangle \overset{\text{def}}{=} [|001\rangle + |010\rangle + |100\rangle]/\sqrt{3}$. Again, after some tedious but straightforward calculations, it turns out that the curvature κ_{AC}^2 and torsion τ_{AC}^2 coefficients become

$$
\kappa_{\text{AC}}^2 (J_x, J_y, J_z, h) = \frac{4}{3} \frac{(2h + J_x + J_y - 2J_z)^2}{(J_x - J_y)^2}, \text{ and } \tau_{\text{AC}}^2 (J_x, J_y, J_z, h) = 0, \tag{C8}
$$

respectively. From the expressions of the curvature coefficients in Eq. (C4) and the first relation in Eq. (C8), we see that curves traced by the $|GHZ\rangle$-state and the $|W\rangle$-state are differently bent by the driving Hamiltonian. Moreover, from Eq. (C5) and the second relation in Eq. (C8) we observe that while the driving Hamiltonian in Eq. (C3) can twist the quantum curve traced by the $|GHZ\rangle$-state, it cannot twist the curve traced by the $|W\rangle$-state. These distinct curvature and torsion behaviors under the same driving Hamiltonian are interesting. Indeed, it is known that the $|GHZ\rangle$-state and the $|W\rangle$-state cannot be transformed into each other by local quantum operations. Therefore, they represent very different types of tripartite entanglement. The curvature and torsion coefficients seem to detect this difference. However, a more comprehensive investigation would be necessary to fully understand these behaviors.